

TRIESTE / ICTP
17-22 Sept. '90

L. RAMELLO

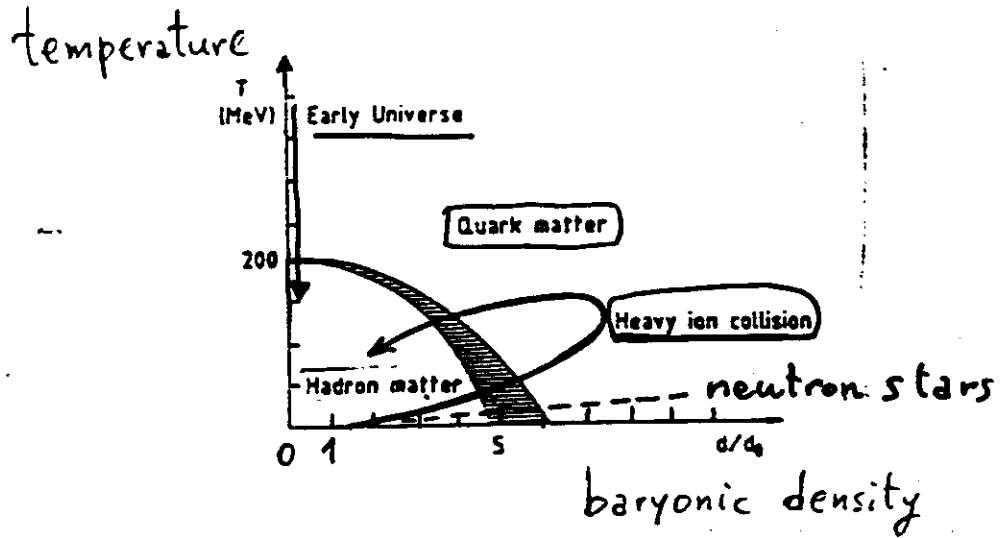
RELATIVISTIC HEAVY-ION SCATTERING EXPERIMENTS

- I. Physics interest
- II. Beams & experiments
- III. Results on global features E_T , N_{CH}
- IV. Results on p_T , particle ratios flow, equilibration
- V. Results on π interferometry source size
- VI. Results on dileptons J/ψ suppression

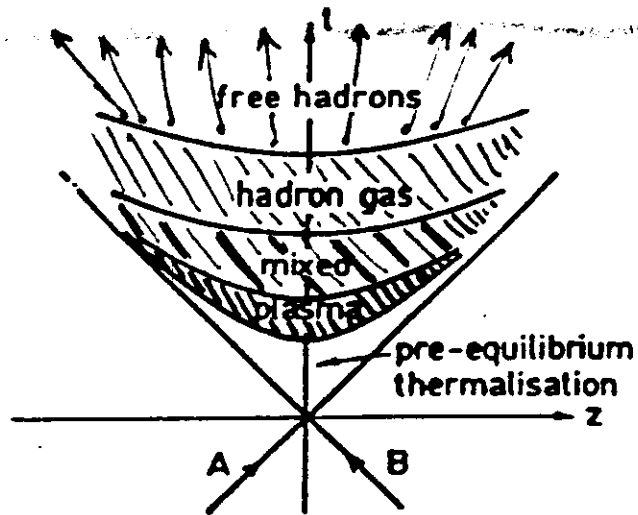
I. PHYSICS INTEREST

- STUDY OF NUCLEAR MATTER AT HIGH TEMPERATURE AND/OR DENSITY OVER "LARGE" VOLUMES, I.E. STRONG INTERACTION THERMODYNAMICS
 - LATTICE QCD CALCULATIONS SUPPORT A PHASE TRANSITION TO QUARK-GLUON PLASMA (QGP) LINKED TO DECONFINEMENT AND CHIRAL SYMMETRY RESTORATION
 - EQUATION OF STATE OF DENSE NUCLEAR MATTER
 - LINKS TO COSMOLOGY & ASTROPHYSICS:
EARLY UNIVERSE (10^{-5} s AFTER BIG BANG)
NEUTRON STARS, BLACK HOLES
- * SIGNATURES OF QGP FORMATION ARE OBSCURED BY THE SUBSEQUENT COOLING AND HADRONIZATION, SO ONE NEEDS TO UNDERSTAND SIMULTANEOUSLY A-A, p-A AND \bar{p} p DATA TO ISOLATE SIGNATURES OUT OF TRIVIAL SUPERPOSITION OF NUCLEON-NUCLEON INTERACTIONS
- * TO THIS EFFECT AN EXTENSIVE USE IS MADE OF QCD-INSPIRED MONTE CARLO GENERATORS

PHASE DIAGRAM



SPACE-TIME PICTURE



- LATTICE QCD CALCULATIONS INDICATE A FIRST ORDER PHASE TRANSITION FROM HADRON GAS TO QGP, BOTH FOR PURE GAUGE THEORY ($N_F=0$) AND WITH 2 OR 4 DEGENERATE QUARK FLAVORS
- THE NATURE OF THE TRANSITION DEPENDS ON THE RATIO m_q/T : IT IS "CHIRAL" FOR $m_q/T \leq 0.1$, AND OF DECONFINEMENT TYPE FOR $m_q/T > 1$
- THE CRITICAL TEMPERATURE T_c IS ≤ 200 MeV, DECREASING AS N_F INCREASES
- THE JUMP IN ENERGY DENSITY (AND ENTROPY DENSITY) AT $T = T_c$ IS CLOSE TO THE DIFFERENCE OF STEFAN-BOLTZMANN VALUES BETWEEN A HADRON GAS ($g_h = 3$ FOR MASSLESS PIONS) AND A GAS OF FREE QUARKS AND GLUONS
- THE CRITICAL ENERGY DENSITY ϵ_c IS PROPORTIONAL TO T_c^4 , SO ITS NUMERICAL VALUE HAS LARGE UNCERTAINTY:

$$\epsilon_c \approx 1 \div 3 \text{ GeV/fm}^3$$

recall:

$$\epsilon = 0.15 \text{ GeV/fm}^3 \text{ IN NUCLEI}$$

$$\epsilon = 0.5 \text{ GeV/fm}^3 \text{ IN NUCLEONS}$$

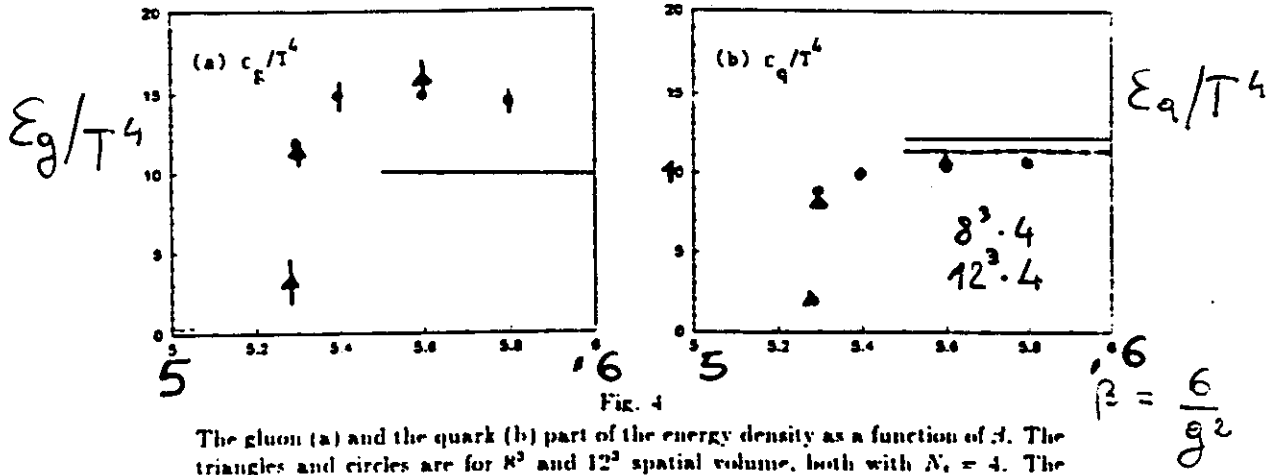


FIG. 4

The gluon (a) and the quark (b) part of the energy density as a function of β . The triangles and circles are for 8^3 and 12^3 spatial volume, both with $N_t = 4$. The lines are weak-coupling prediction to order g^2 on the same size of the lattice (solid for 8^3 and dashed for 12^3). For the gluon part, the two lines overlap. From ref. 42.

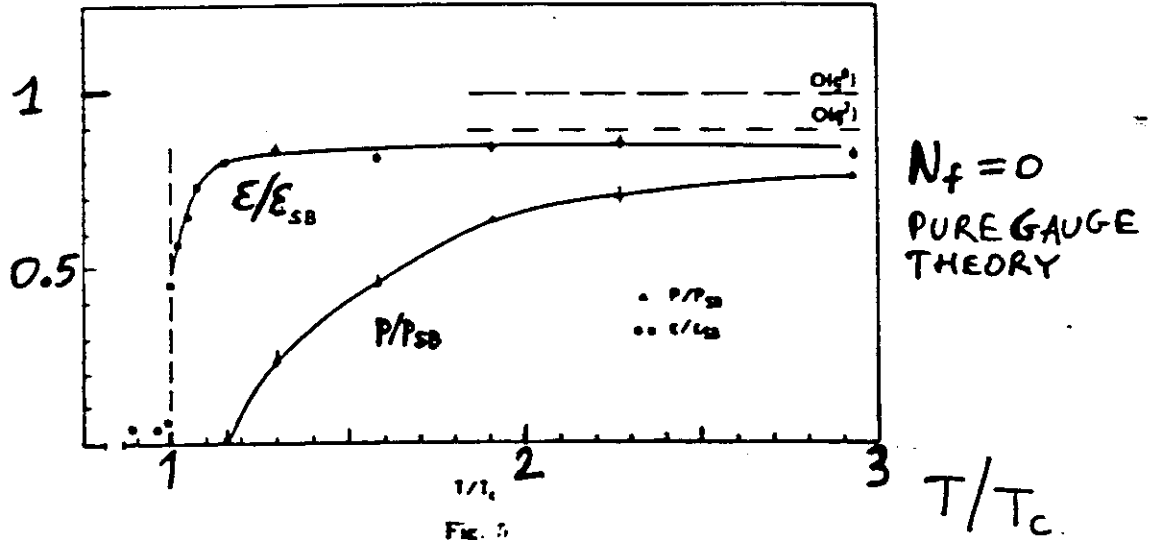
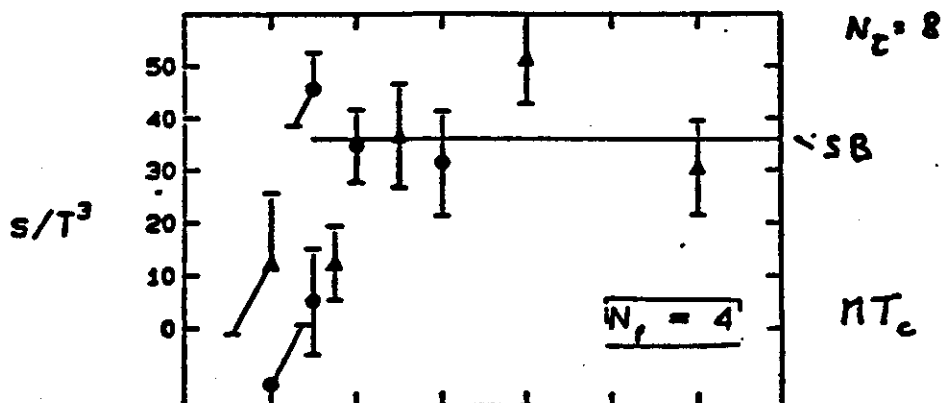
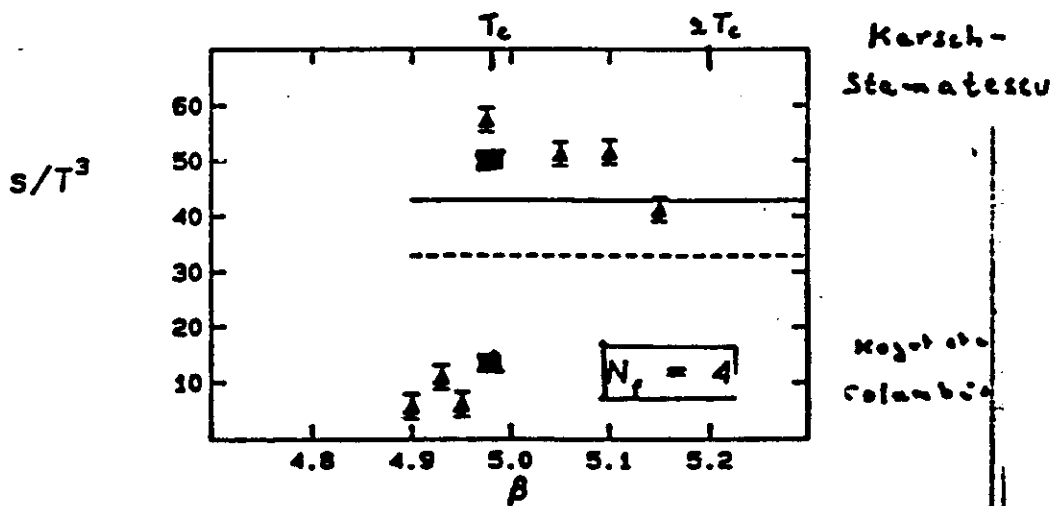
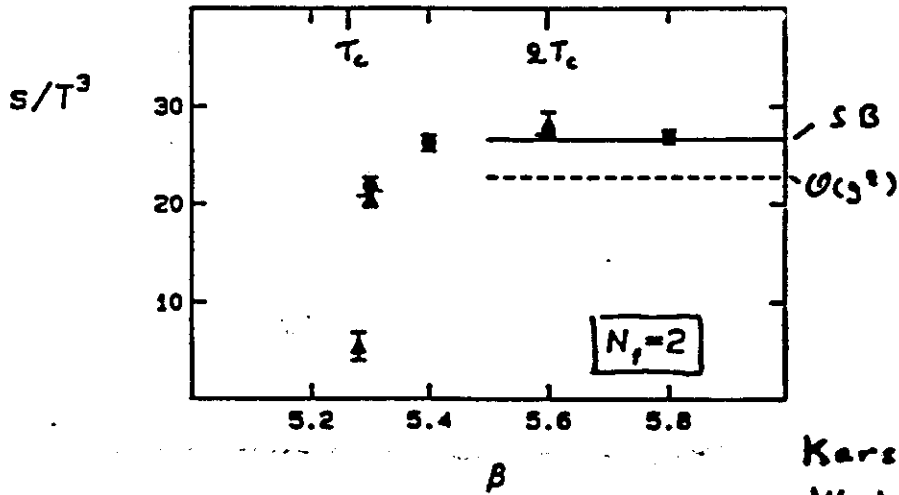
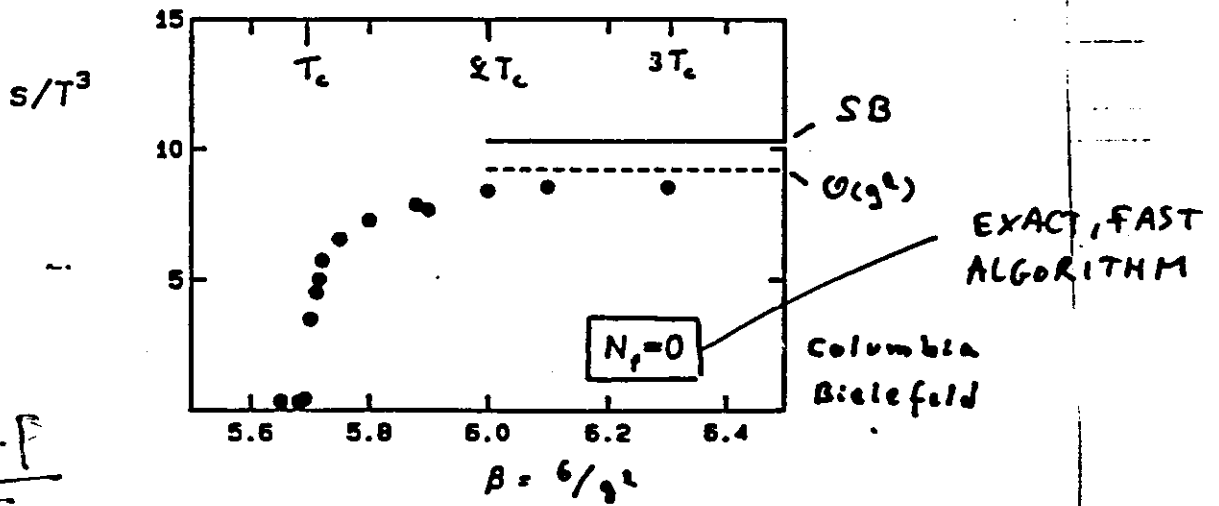


FIG. 5

The gluon energy density and the pressure in the pure gauge theory normalized by the lowest order lattice weak-coupling value. The ratio T/T_c takes into account empirical violation of scaling. The circles and triangles are from ref. 45 ($12^3 \times 4$), and the squares from ref. 46 ($24^3 \times 4$). The latter assumed $p = 0$ to obtain the energy density. From F. Karsch⁴⁴.

Petersson QM '90

$$S = \frac{C + F}{T}$$



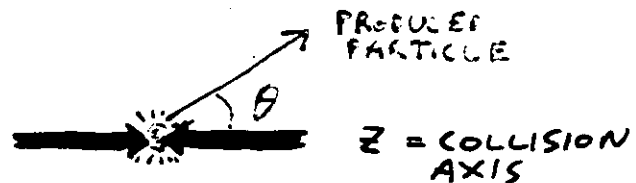
KINEMATICS

- ONE-PARTICLE INCLUSIVE DISTRIBUTIONS ARE OFTEN MEASURED IN TERMS OF RAPIDITY:

$$y = \frac{1}{2} \ln \frac{1 + \beta_z}{1 - \beta_z} \equiv \frac{1}{2} \ln \frac{E + p_z}{E - p_z}$$

AND TRANSVERSE MOMENTUM:

$$p_T = p \sin \theta$$

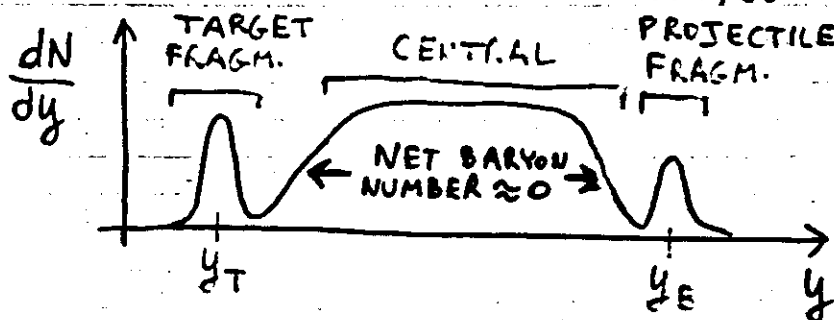


- THE RAPIDITY y TRANSFORMS ADDITIVELY FOR LONGITUDINAL LORENTZ BOOSTS WITH VELOCITY β'_z :

$$y' = y + \tanh^{-1}(\beta'_z)$$

(NOTE THAT $\beta_z = \tanh y$), SO DISTRIBUTIONS IN y ARE INVARIANT IN FORM WHEN GOING, E.G., FROM THE C.M. TO THE LABORATORY SYSTEM.

- OBSERVED PARTICLES ARE CLASSIFIED IN 3 REGIONS:



THE SEPARATION $|y_B - y_T|$ INCREASES LOGARITHMICALLY WITH BEAM ENERGY (AT SPS, 200 GeV/N, IT'S ~ 6 UNITS).

- RAPIDITY IS OFTEN APPROXIMATED BY AN EASILY MEASURABLE QUANTITY, PSEUDORAPIDITY:

$$\eta = -\ln(\tan \theta/2) \equiv \frac{1}{2} \ln \frac{p + p_z}{p - p_z}$$

FOR RELATIVISTIC PARTICLES ($p \approx E$) ONE HAS $\eta \approx y$.

- * BJORKEN MODEL (LONGITUDINAL, BOOST-INVARIANT HYDRODYN. EXPANSION) PREDICTS RAPIDITY PLATEAU IN THE CENTRAL

CONDITIONS NEEDED TO PRODUCE QGP:

- * HIGH ϵ BY COMPRESSION AND/OR HEATING
→ RELATIVISTIC PROJECTILES
- * LARGE VOLUMES / LIFETIMES TO HAVE A THERMODYNAMICAL SYSTEM
→ HEAVY IONS

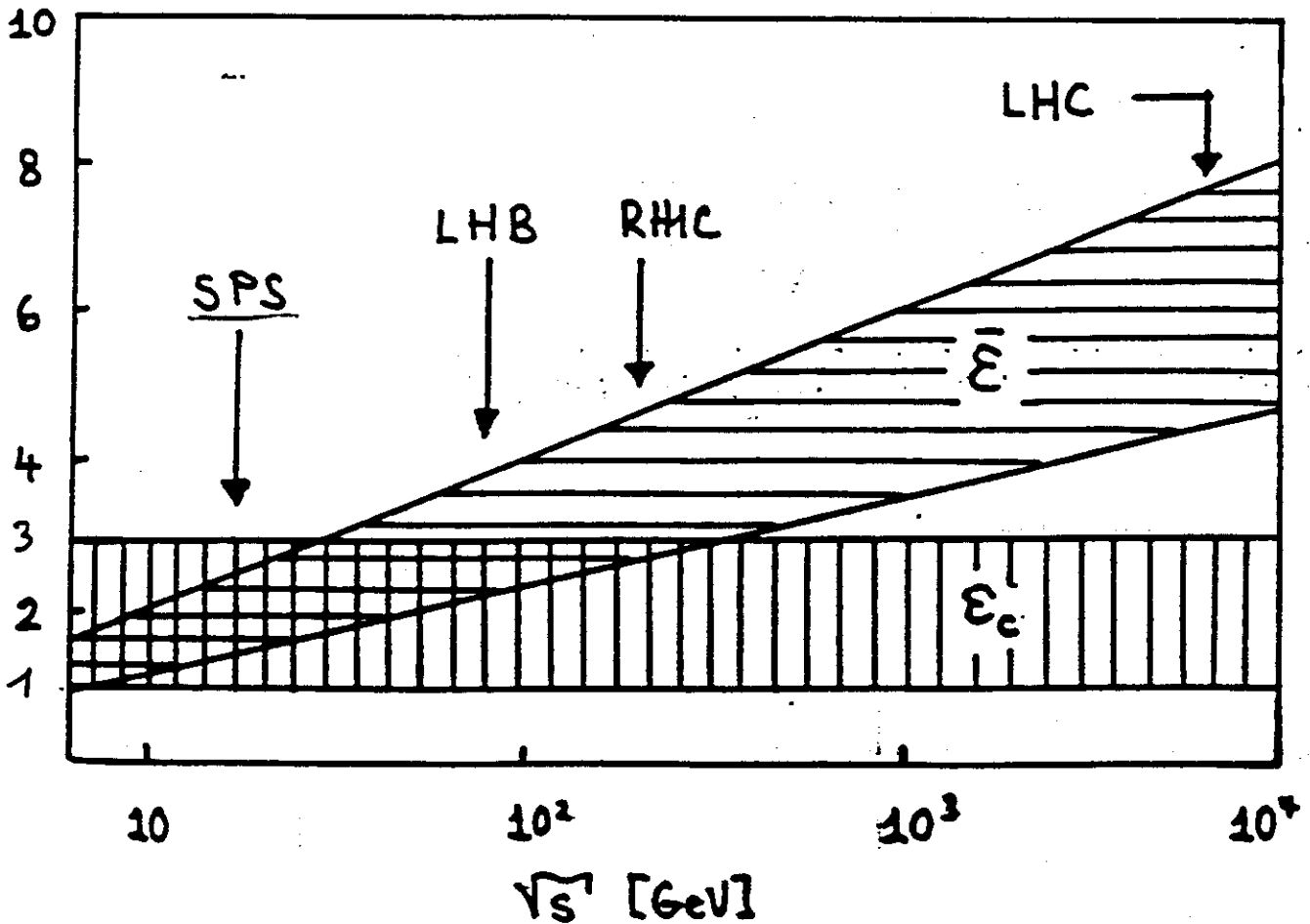
THESE CONDITIONS ARE "VERIFIED" BY STUDYING GLOBAL FEATURES LIKE TRANSVERSE ENERGY AND MULTIPLICITY → SECTION III

SPECIFIC SIGNATURES:

- ◆ EQUILIBRATION, COLLECTIVE FLOW
→ via P_{\perp} spectra, particle ratios ($K/\pi, \dots$)
 $\langle P_{\perp} \rangle$ vs. dN/dy → SECTION IV
- ◆ SOURCE SIZE (AND LIFETIME)
→ via HBT interferometry → SECTION V
- ◆ PARTICLES EMITTED BY QGP IN EARLY STAGES
→ thermal photons, dileptons
- ◆ "MELTING" OF HEAVY $q\bar{q}$ STATES
→ $J/\psi, \psi', \Upsilon, \dots$ suppression → SECTION VI
- ◆ RAPIDITY FLUCTUATIONS (JACEE)
- ◆ INTERMITTENCY ?

Bjorken average ϵ for central Pb-Pb collisions

$$\epsilon \text{ [GeV/fm}^3] \approx 0.0884 A^{\alpha-2/3} \ln \sqrt{s} ; A=208, \alpha=1.0 \div 1.1$$



$$\epsilon = \frac{\langle m_T \rangle}{\pi R^2 \tau} \left(\frac{dN}{dy} \right)$$

$m_T = \text{transverse mass} \approx 0.5 \text{ GeV}$

$R = r_0 A^{1/3} \quad r_0 \sim 1.2 \text{ fm}$

$\tau = \text{formation length} \sim 1 \text{ fm}$

$$\left(\frac{dN}{dy} \right)_{AA} = A^\alpha \left(\frac{dN}{dy} \right)_{pp}$$

II. BEAMS AND EXPERIMENTS

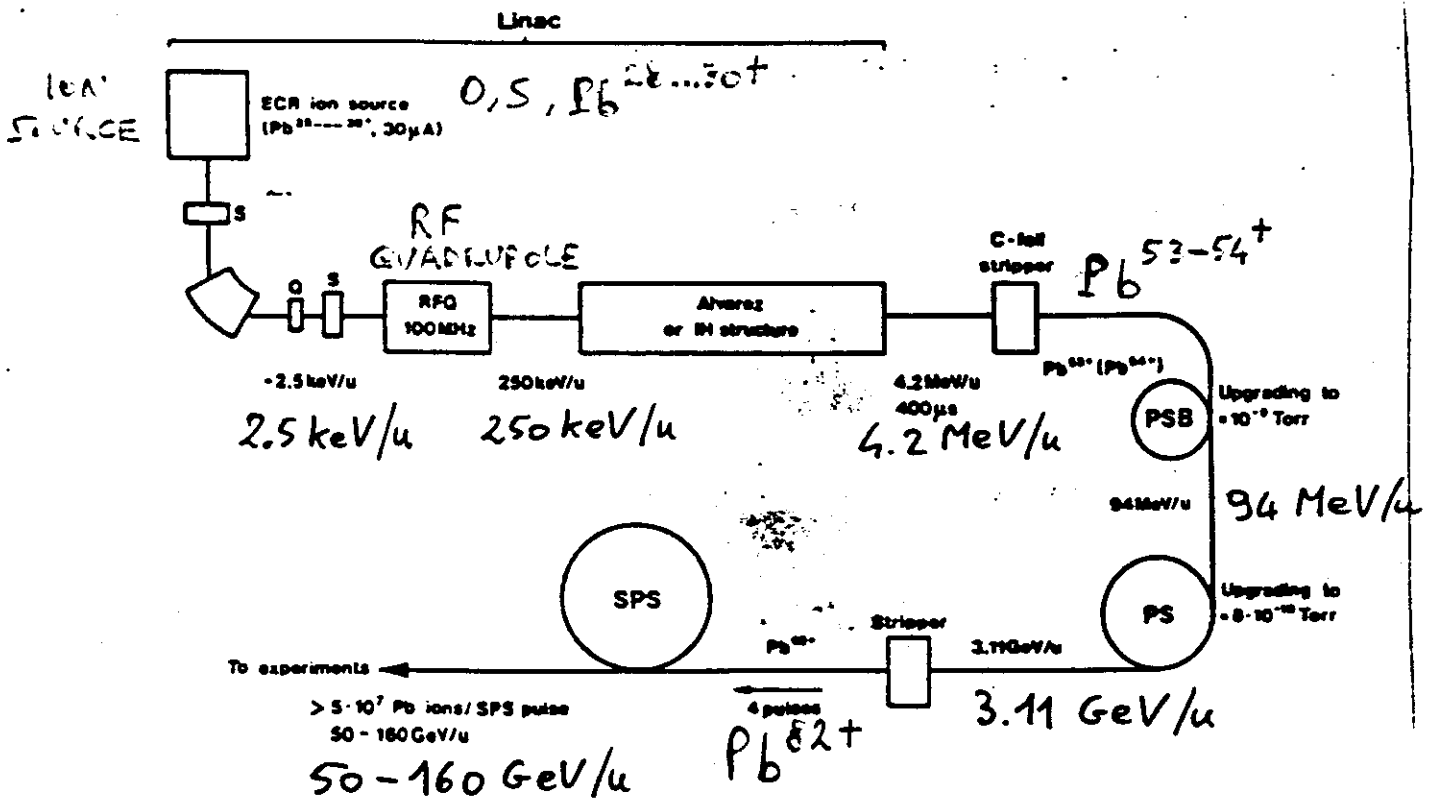
PRESENT AND FUTURE ACCELERATORS:

	IONS	E/nucleon GeV	$\sqrt{s_{NN}}$ GeV	INTENSITY ions/pulse	AVAILABLE FROM
BNL/AGS	upto ^{28}Si	14.5	5	10^9	1986
CERN/SPS	$^{16}\text{O}, ^{32}\text{S}$	60/200	10/19	$10^9/5 \times 10^7$	1986/87
BNL/AGS BOOSTER	upto ^{197}Au	14.5	5	$10^8 - 10^9$	1991
CERN/SPS	upto ^{208}Pb	160	17	4×10^8	1993 ?
BNL/RHIC	upto ^{197}Au	100	200	$L = 2 \times 10^{26}$	1997 ?
CERN/LHC	upto ^{208}Pb	3150	6300	$L = 10^{27}$	1998 ?

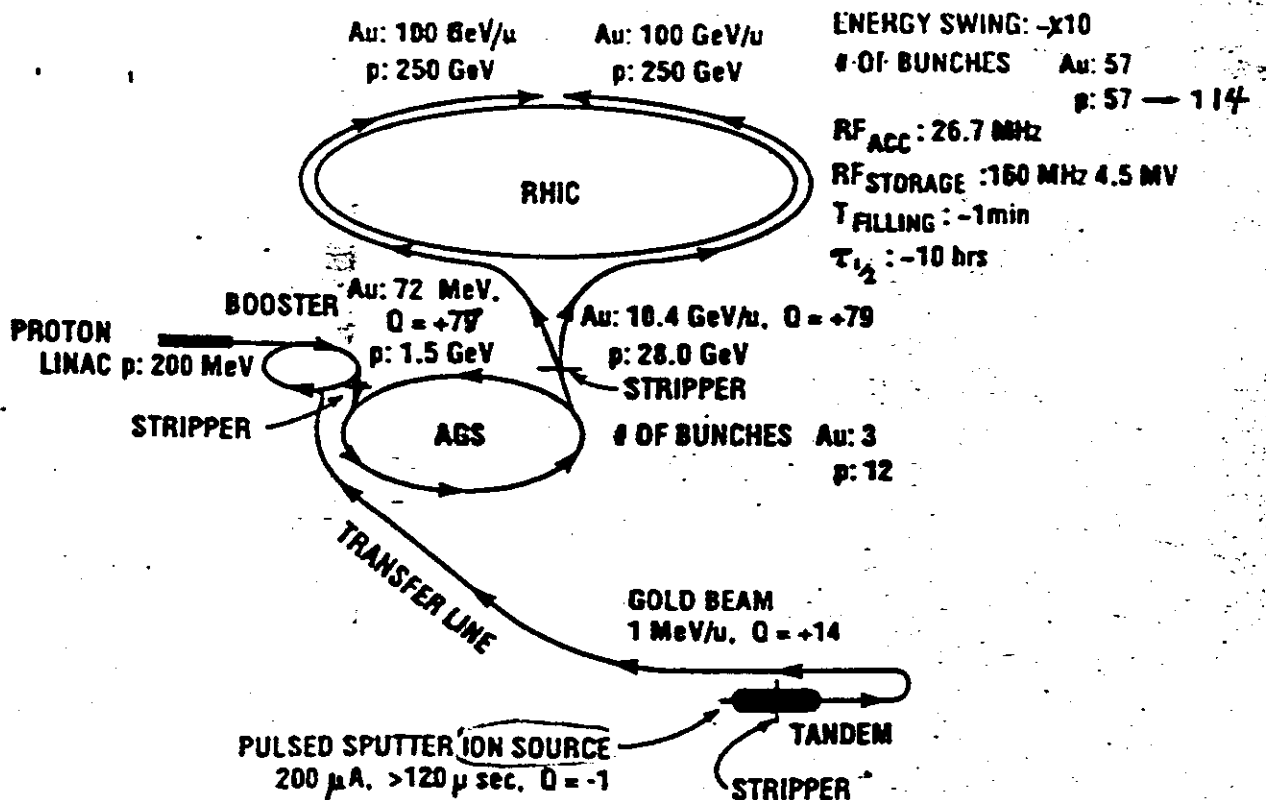
BNL/AGS EXPERIMENTS:

EXPERIMENT	DETECTOR	MEASURES
E802	ZERO DEGREE CALORIM. Pb-GLASS CALORIM. MAGN. SPECTROM.	E_{20} dE_T/dM $p, \bar{p}, d, \pi^\pm, K^\pm$
E810	TIME PROJECTION CHAMBER	p, θ of charged particles
E814	NaI/U CALORIMETER TARGET CALORIM. SILIC. N. MULT. CTR. PARTICIPANT CALD. FORWARD SPECTROM. AND CALORIMETER	E_T, N_{ch} neutrons and protons in forward direction

CERN LINAC - PS - SPS COMPLEX



BNL RHIC ACCELERATION CONFIGURATION



CERN/SPS EXPERIMENTS :

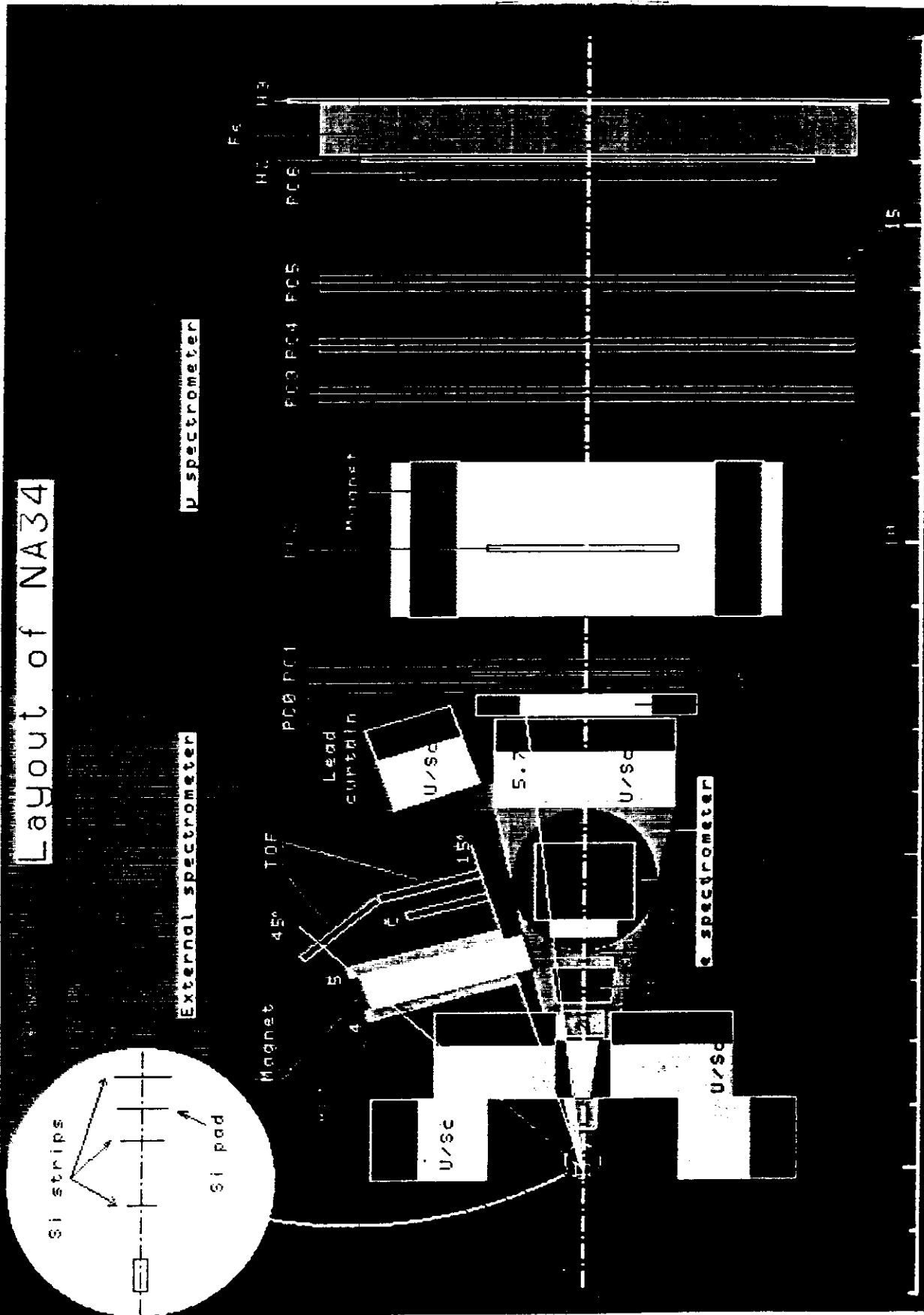
EXPERIMENT	DETECTOR	MEASURES
NA34 (HELIX)	U/S.C. CALORIMETER U/Liq. Ar CALORIM. SILICON COUNTERS EXTERNAL SPECTROM. MUON SPECTROM.	$E_T, dE_T/d\eta$ $dN^{ch}/d\eta$ $\pi^\pm, k^\pm, \bar{p}, \gamma$ LOW MASS MUON PAIRS
NA35	ZERO DEGREE CALORIM. RING CALORIMETER PHOTON POSITION DET. STREAMER CHAMBER	E_{ZD}, E_T $\pi^\pm, p, k^0, \Lambda, \bar{\Lambda}$
NA37	TIME PROJECTION CHAMBER	$k^0, \Lambda, \bar{\Lambda}, \Xi, \Omega$
NA38	E.M. CALORIMETER MUON SPECTROMETER	E_T $\mu\mu$ (HIGH MASS)
WA80	ZERO DEGREE CALORIM. MID-RAPIDITY CALORIM. MULTIPLICITY DETECTORS Pb-GLASS PHOTON DET.	E_{ZD}, E_T $N_{CH}, dN^{CH}/d\eta$ γ, π^0
WA85	" Ω " SPECTROMETER	$k^0, \Lambda, \bar{\Lambda}, \Xi$
NA44*	FOCUSSED SPECTROM.	INTERFEROMETRY WITH π, k, \bar{p}
NA45*	e^+e^- SPECTROMETER WITH RICH'S	LOW MASS e^+e^-

* FIRST RUN : AUGUST 1990

IN ADDITION, A LARGE NUMBER OF "SMALL" EXPERIMENTS USE EMULSIONS AND/OR PLASTICS TO MAKE A GENERAL SURVEY OF INTERACTIONS (NO TRIGGER IS USED).

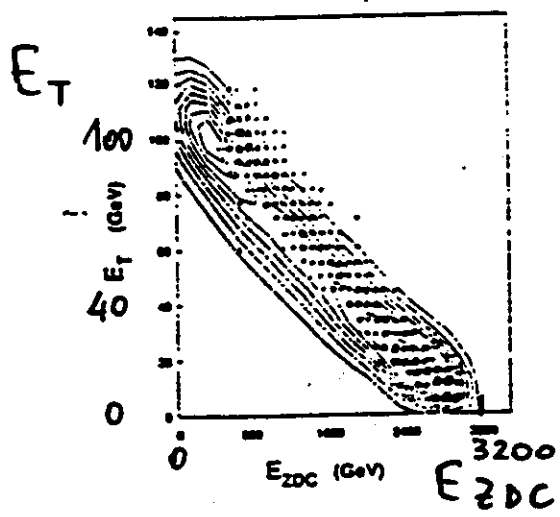
THE HELIX-EMULSION COLLABORATION COMBINES NUCLEAR EMULSIONS WITH THE NA34 APPARATUS.

Layout of NA34



WA80

200 A GeV $^{16}\text{O} + ^{197}\text{Au}$



E_T, N_{CH} ARE
ANTICORRELATED
WITH E_{ZDC}

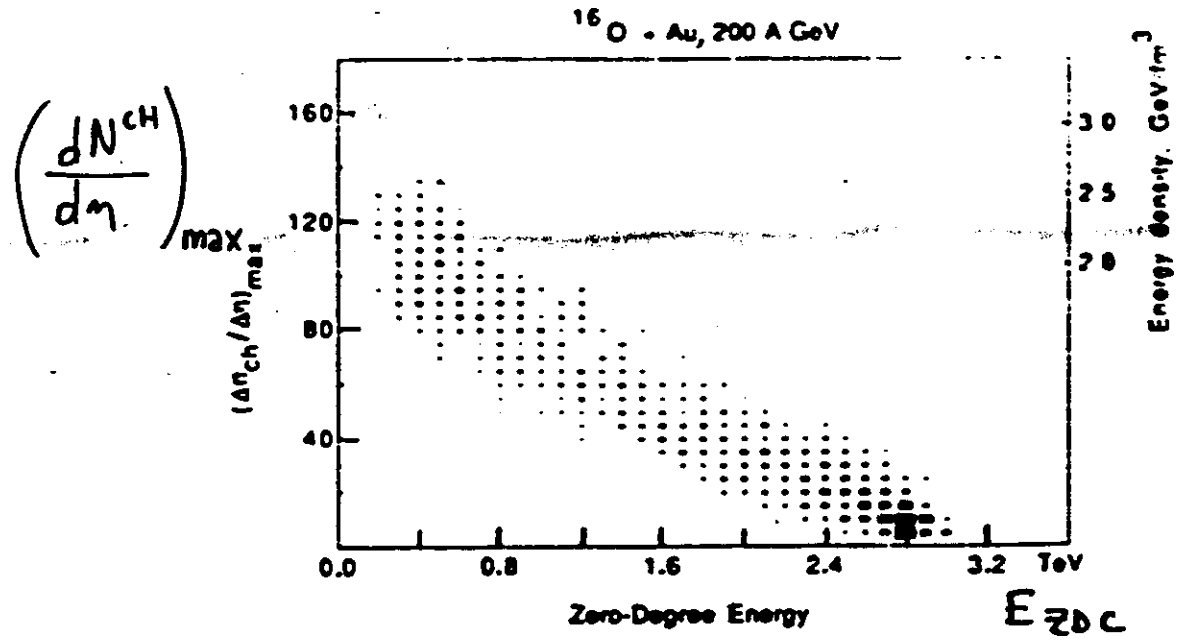


Fig. 8. The density of charged particles in the pseudo-rapidity interval $2.65 < \eta < 3.15$ for $^{16}\text{O} + \text{Au}$ at 200 A GeV. $(\Delta n_{ch}/\Delta \eta)_{max}$, as a function of the energy measured in the ZDC, E_{ZDC} . On the scale to the right we show the corresponding energy densities, derived as described in the text

DIFFERENTIAL CROSS SECTIONS.

- CROSS-SECTIONS IN E_T AND N_{CH} HAVE BEEN MEASURED FROM MANY EXPERIMENTS ON A VARIETY OF NUCLEI, BOTH AT BNL AND CERN ENERGIES: → FIG.

THEY ARE ESSENTIALLY UNDERSTOOD ON THE BASIS OF RATHER SIMPLE GEOMETRICAL MODELS.

- ▶ nucleus-nucleus collision = superposition of N effective nucleon-nucleon interactions, where N is calculated via the overlap integral Ω of the two nuclear densities at the appropriate impact parameter b → FIG.

- ▶ E_T (or N_{CH}) cross-section fitted with 2 free parameters:

$$\epsilon_c = \text{average } E_T \text{ per nucleon-nucleon int.}$$

$$\omega = \text{variance } / \epsilon_c^2$$

(E_T at a given impact parameter is assumed gaussian distribute with average $N\epsilon_c$ and variance $\omega N\epsilon_c^2$)

RESULTS OF GEOMETRICAL MODEL FITS FOR **HELIOS** $^{32}_S$ DATA AT 200 GeV/N OVER THE LARGEST COVERAGE ($-0.1 < \eta < 5.5$):

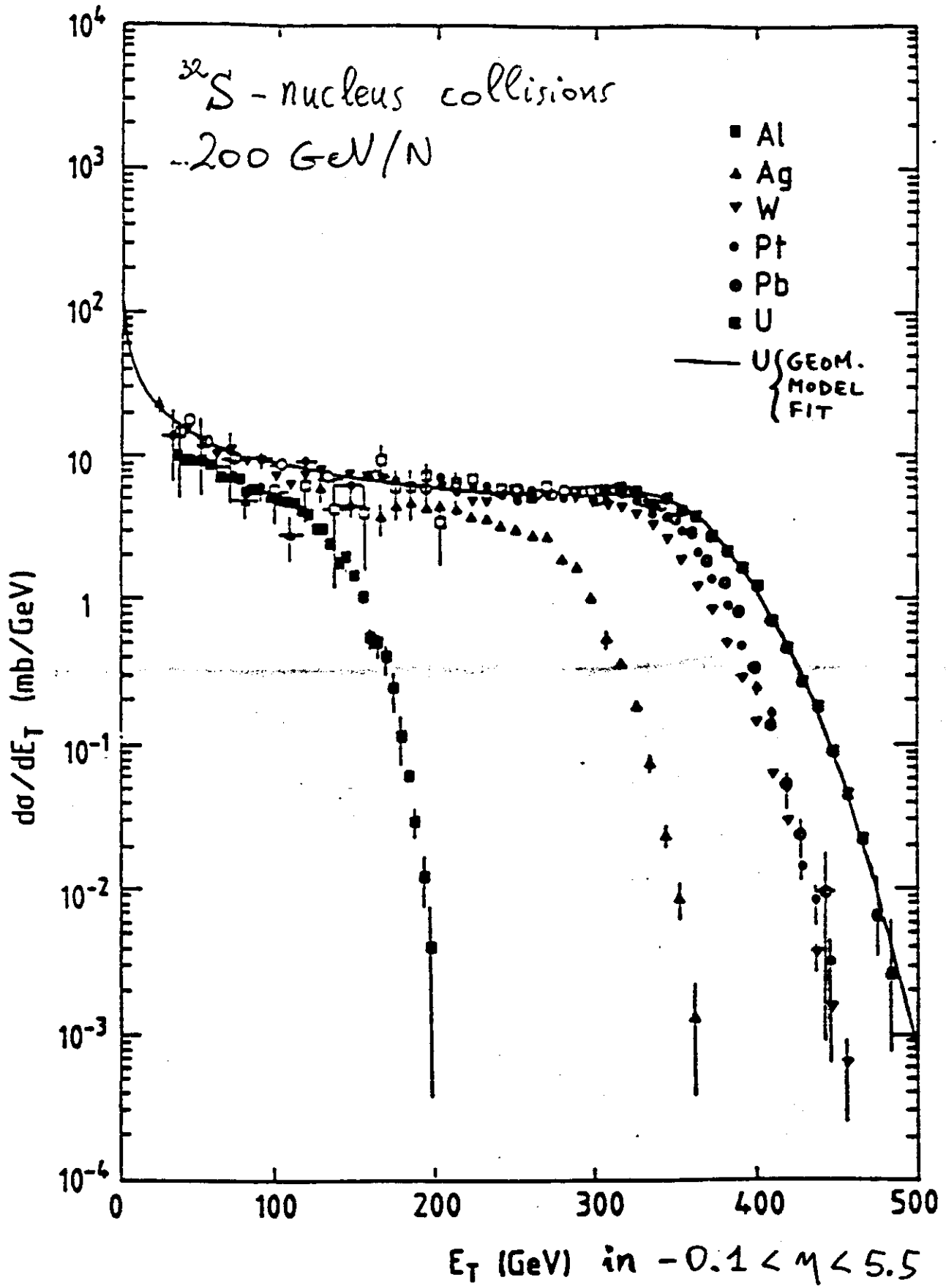
S →	Al	Ag	W	Pb	U
ϵ_c	$1.88 \pm .06$	$1.71 \pm .02$	$1.67 \pm .005$	$1.68 \pm .03$	$1.63 \pm .02$
ω	$1.1 \pm .3$	$1.84 \pm .3$	$1.83 \pm .06$	$1.35 \pm .15$	$2.37 \pm .2$
ω_d	—	0.22	0.81	—	1.75
ω_{true}	1.1	1.62	1.10	1.35	0.62

- ▶ ϵ_c is rather constant for various nuclei (recall that $\langle E_T \rangle \sim 1.4$ GeV in p-p collisions at $\sqrt{s} = 20$ GeV)

- ▶ $\omega_W, \omega_U > \omega_{Ag}$ due to nuclear shape: in high E_T events a non-spherical nucleus is aligned (effective $A \sim 400$ for $^{32}_S \rightarrow ^{238}_U$!).

Values of ω are less dispersed when the effect of nuclear deformation ω_d is taken out.

HELIOS



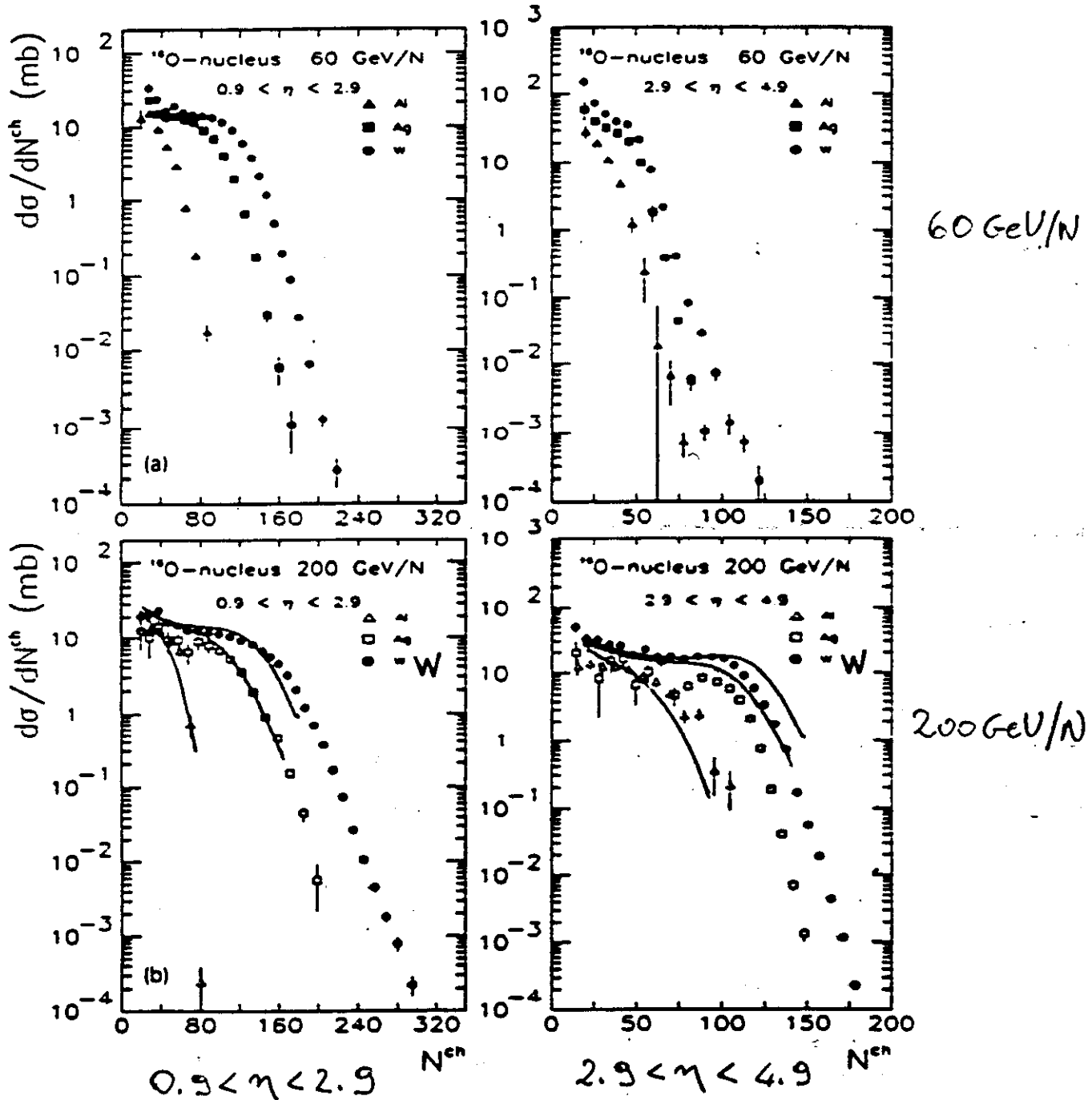


Fig. 3. Charged-particle differential cross section $d\sigma/dN^{ch}$ in the backward and restricted forward regions: (a) at 60 GeV per nucleon, (b) at 200 GeV per nucleon. The error bars are statistical only; the global systematic error on the multiplicity scale is 3%. The lines indicate IRIS predictions.

PSEUDO RAPIDITY DISTRIBUTIONS as a function of "centrality":

$$dN^d/d\eta$$

HELIOS

T. Åkesson et al. / Multiplicity distributions

61

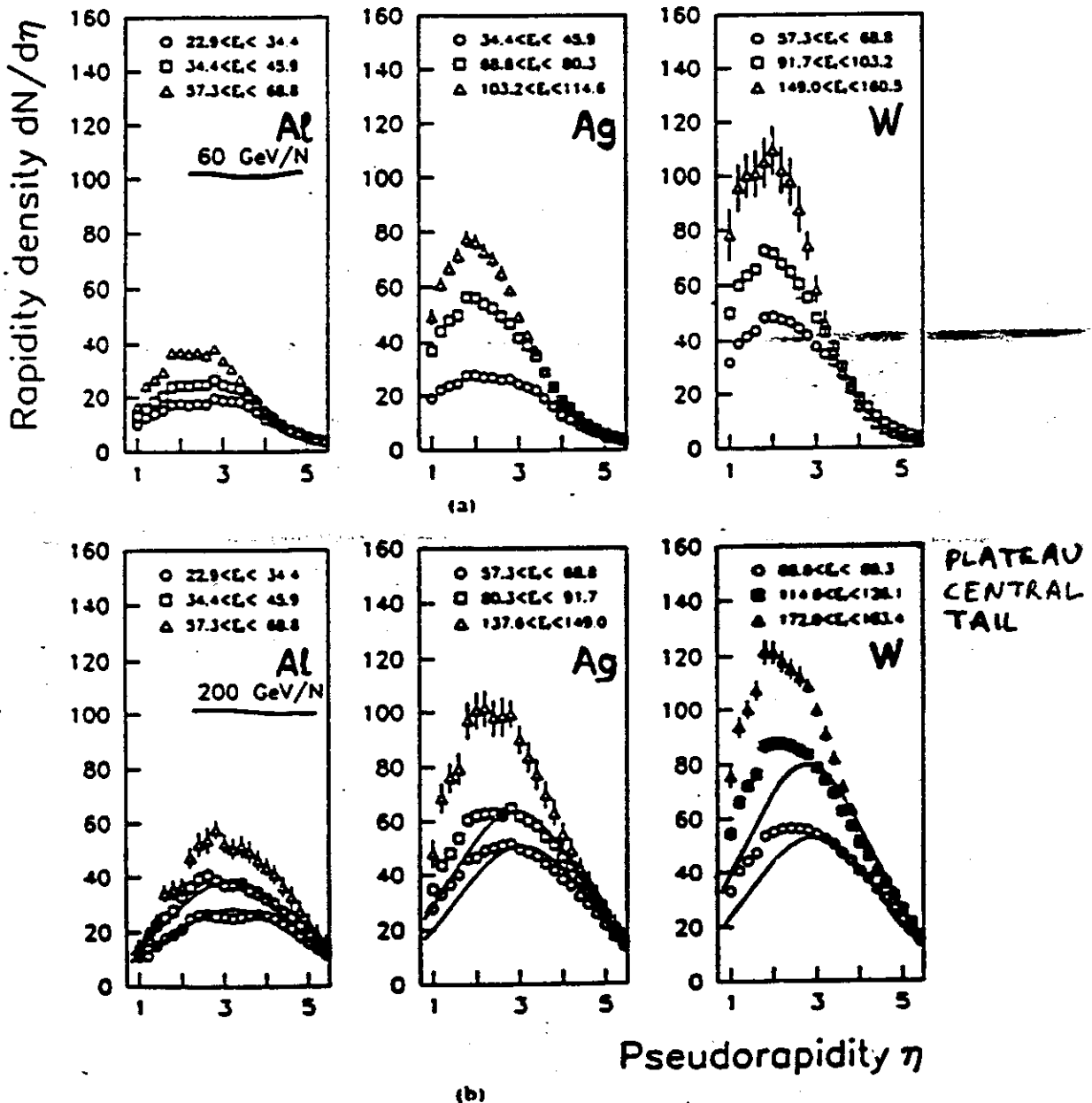


Fig. 4. Distribution of pseudorapidity density for three selected windows in E_T within the trigger region: (a) at 60 GeV per nucleon; (b) at 200 GeV per nucleon. The errors shown are statistical only. The lines indicate IRIS predictions.

(centrality selected by "backward" E_T ($-0.1 < \eta < 2.9$))

- NO RAPIDITY PLATEAU, DISTRIBUTIONS VERY CLOSE TO GAUSSIANS (AS PREDICTED BY LANDAU HYDRODYN. MODEL).

MOMENTS OF $dN^{ch}/d\eta$ DISTRIBUTIONS:

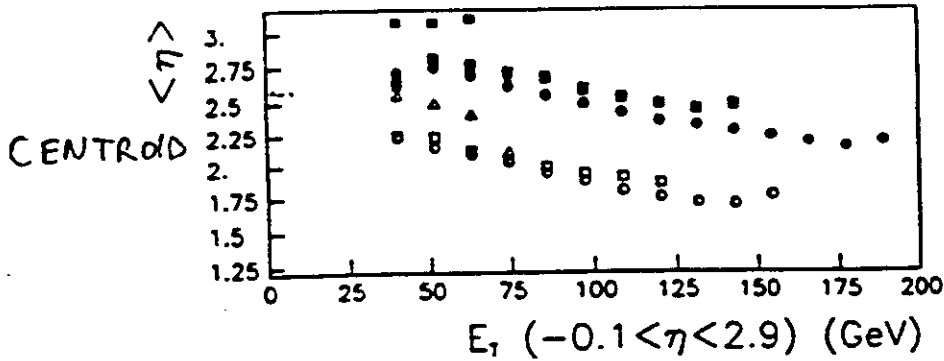
HELIOS

60 GeV 200 GeV

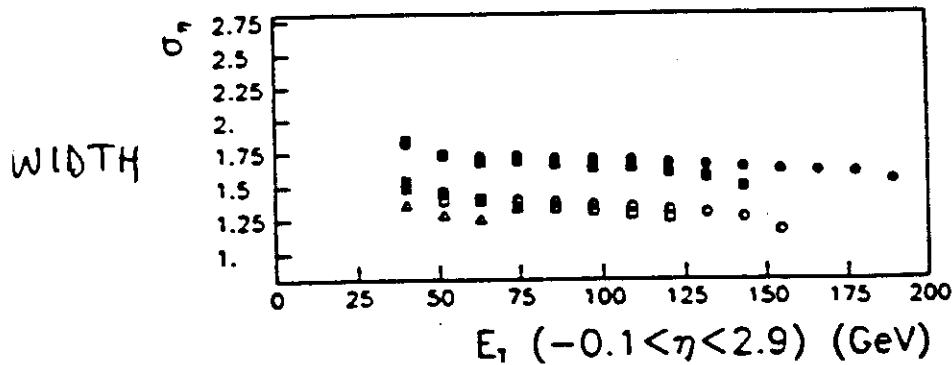
O+AL \triangle \blacktriangle
 Ag \square \blacksquare
 W \circ \bullet

62

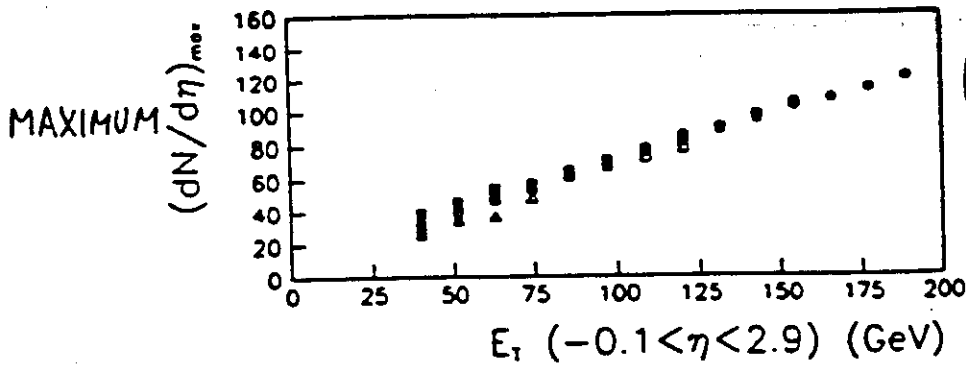
T. Åkesson et al. / Multiplicity distributions



$\langle \eta \rangle$ moves back with increasing centrality due to changing participants' kinematics



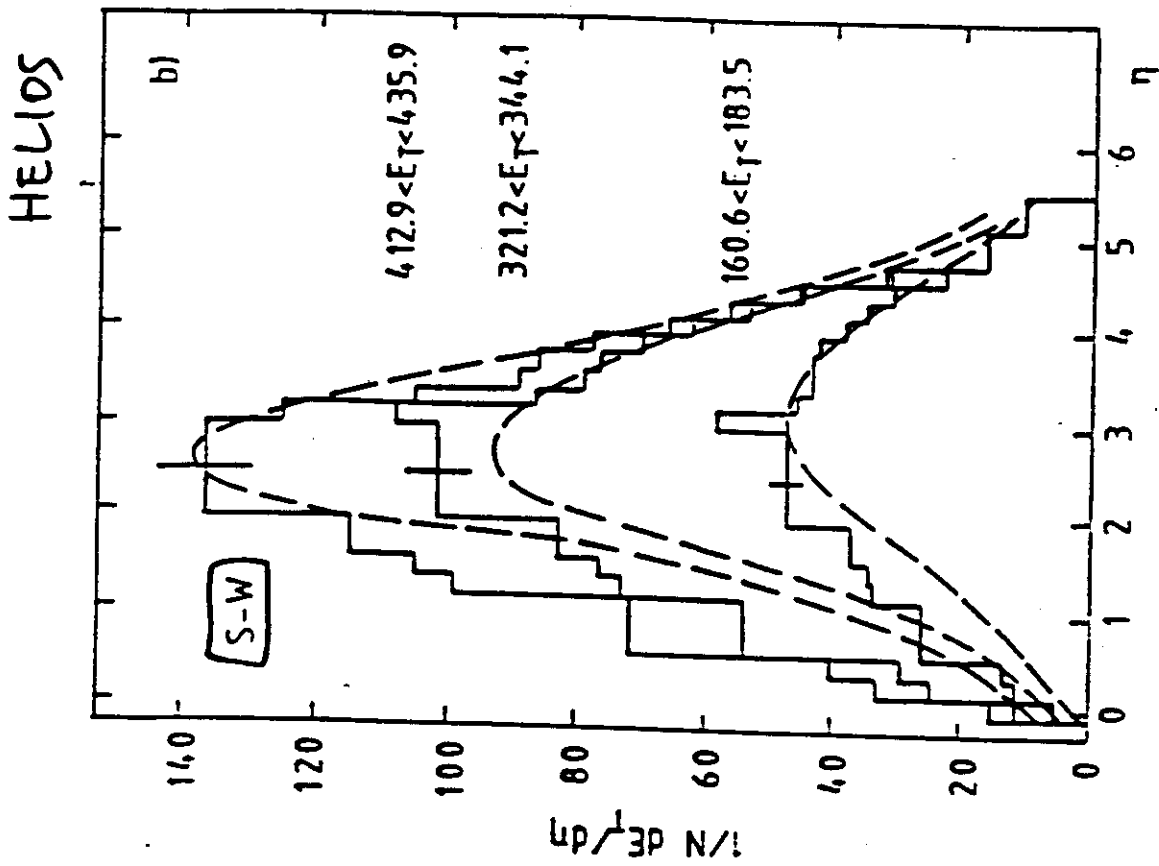
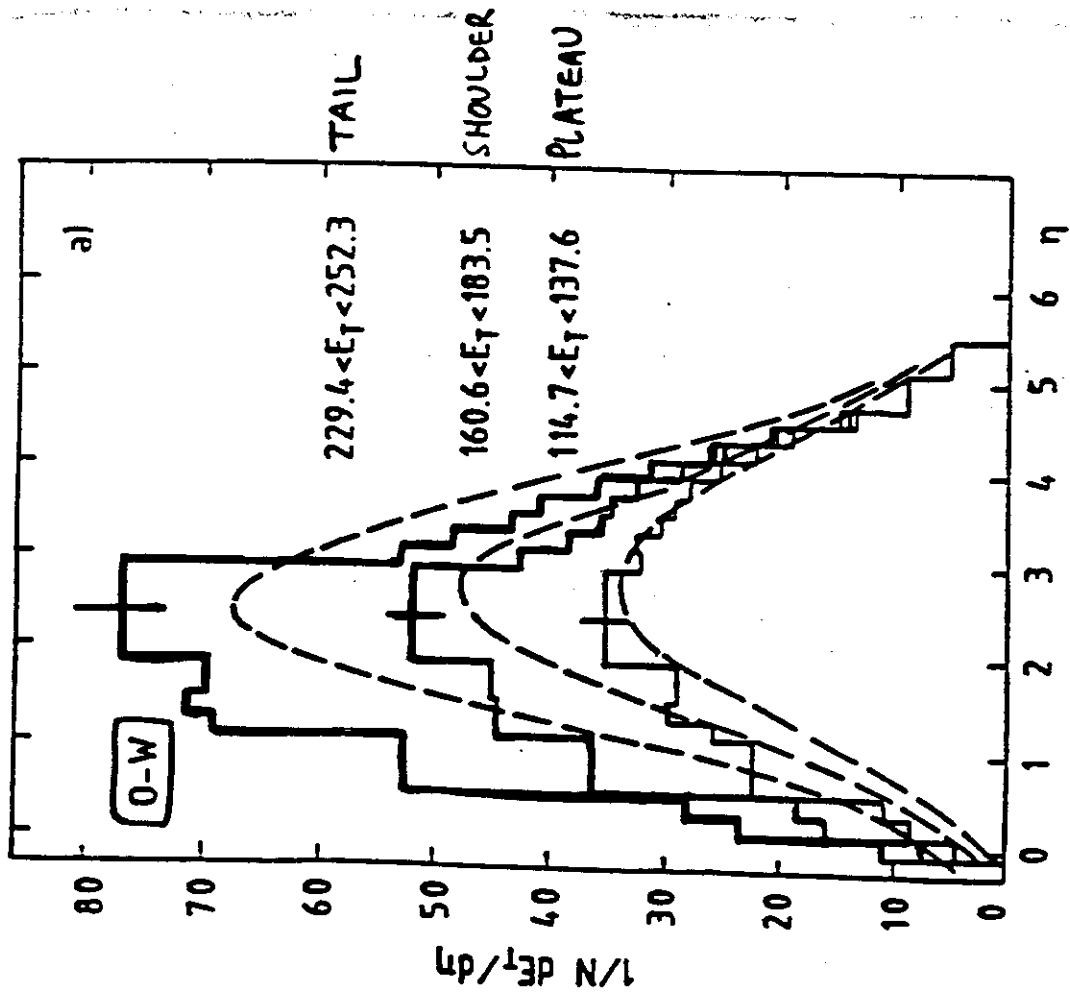
σ_η decreases by about 10% for very central collisions



$(\frac{dN}{d\eta})_{max}$ is very close to linear vs. E_T

Fig. 5. Evolution of mean η , standard deviation, and maximum pseudorapidity density with E_T for Ag targets (squares) and W targets (circles), at 60 GeV (open symbols) and 200 GeV (closed symbols) per nucleon.

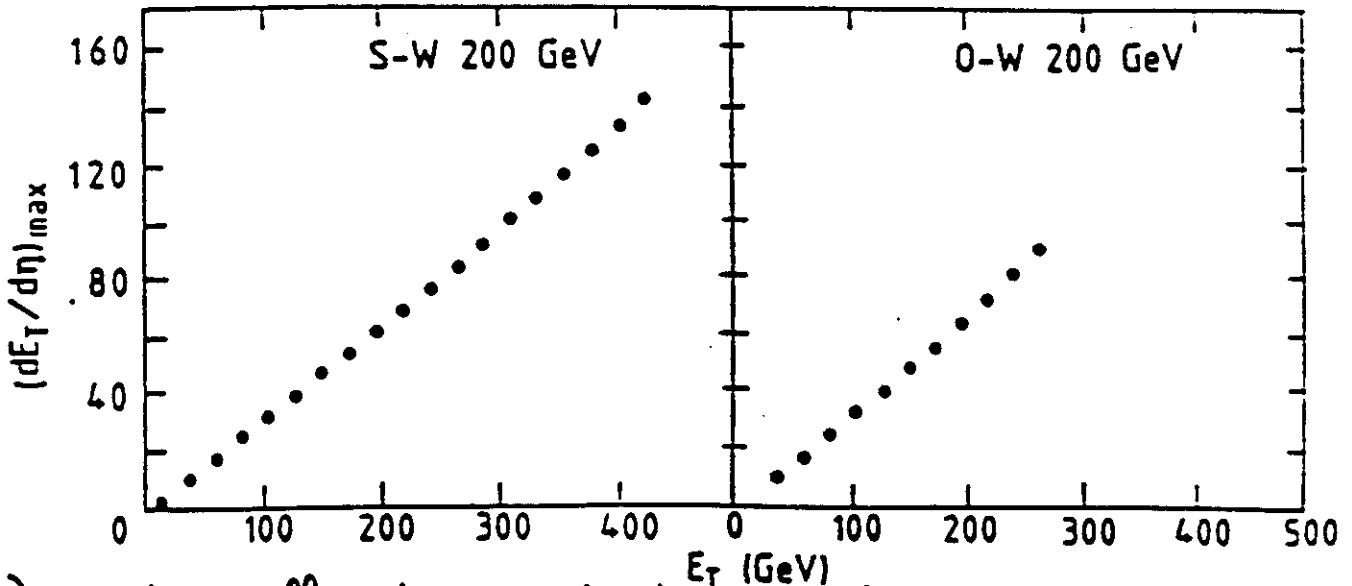
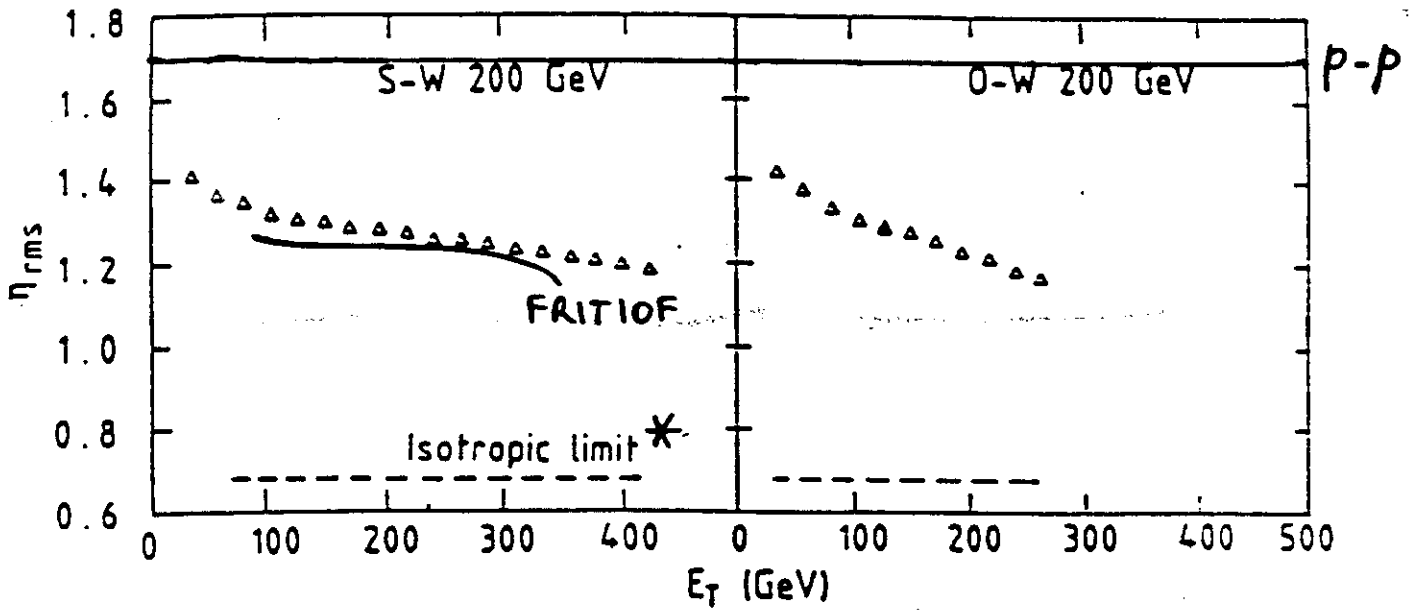
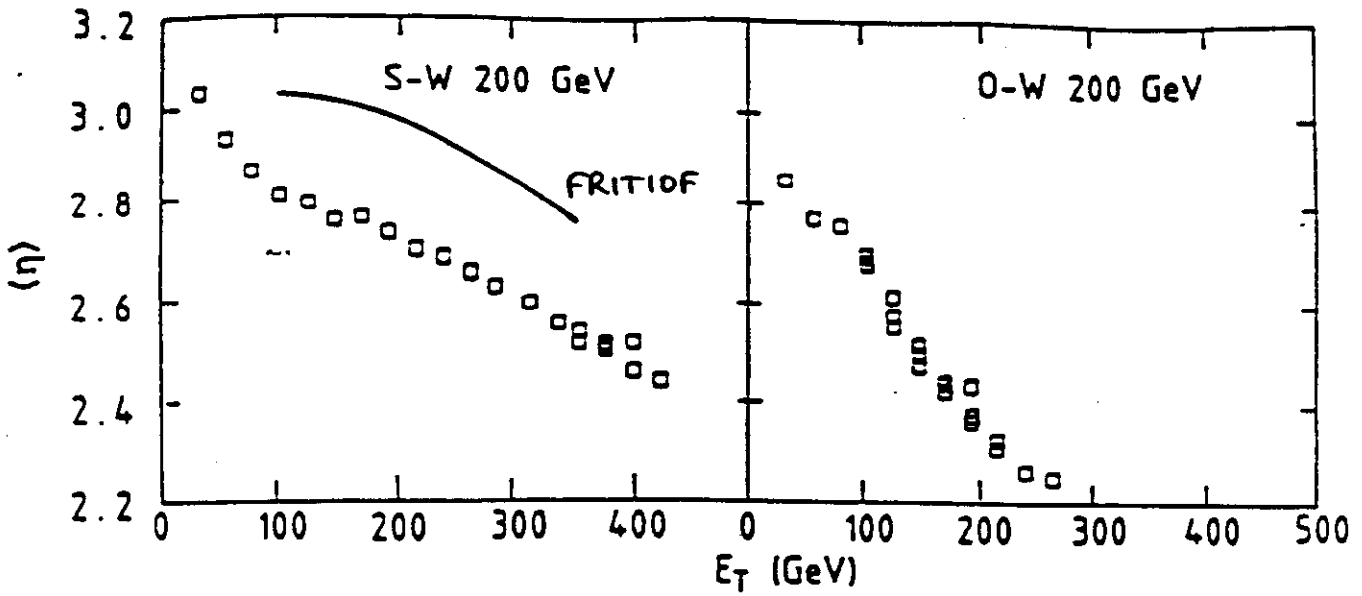
dE_T/dm



--- IRIS at same dE_T/dm value as data

MOMENTS OF $dE_T/d\eta$ DISTRIBUTIONS:

HELIOS



*) Isotropically decaying fireball would give :

$$dE_T \sim 1 \quad \Rightarrow \quad \eta_{rms} = 0.7$$

HELIOS

320
280
240
200
160
120
80
40
0

P_{tot}
(GeV)

$(2.9 < \eta < 5.5)$

S-W collisions
200 GeV/nucleon
two contours separated
by a factor $1/e$

$1.48 \cdot 10^{-1} \text{ mb/GeV}^2$

$2.7 \cdot 10^{-3} \text{ mb/GeV}^2$

10^{-3} mb/GeV^2

IRIS

320 280 240 200 160 120 80 40 0

Forward/backward contour plot

$E_{\text{back}} \text{ (GeV)} (-0.1 < \eta < 2.9)$

for central collisions
 E_T forward
does not increase
any more
while E_T
does.

a still more
target participants?

a independent
production
mechanisms?

EVALUATION OF STOPPING AND ENERGY DENSITY

- Stopping defined via observed E_T :

$$S = \frac{E_T}{E_T^{\max}}$$

where E_T^{\max} is proportional to the available energy
 $E^{\max} = E^{cm} - (A_P + A_T)m_N$ with a coefficient dependent on the assumed "fireball" kinematics:

$$E_T^{\max} = \frac{\pi}{4} E^{\max} \quad \text{isotropic fireball}$$

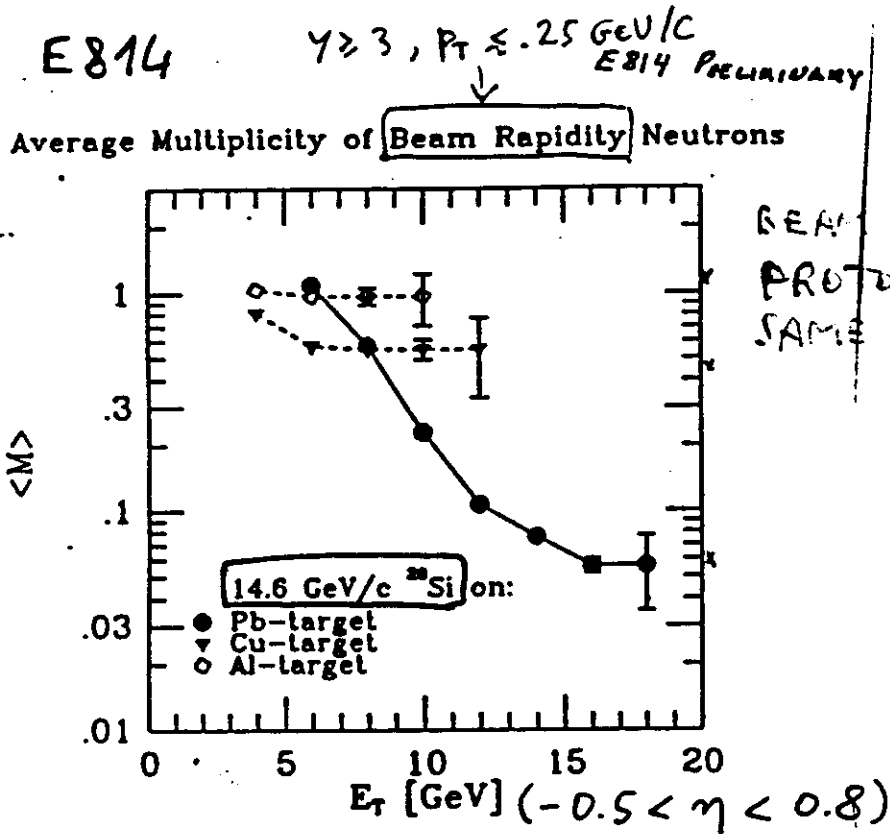
$$c E^{\max} \quad (c < \pi/4) \quad \text{Landau fireball}$$

- **HELIOS** data on stopping fraction $\left\{ \begin{array}{l} E_T \text{ at } d\sigma/dE_T = 10^{-2} \text{ mb/GeV}^* \\ E_T \text{ at } d\sigma/dE_T = 10^{-4} \times \text{PLATEAU} \end{array} \right.$

BEAM ENERGY	TARGET:	Al	Ag	W	
160-60		0.7	0.8	0.9	* dE_T/dm from isotropic fireball
160-200		0.5	0.6	0.7 0.88	♦ dE_T/dm from dat
325-200		0.45 0.56	0.55 0.84	0.65 0.88	

- SFB is probably an underestimate of S (Landau fireball is more realistic)
- stopping decreases with E_{beam} ($S \sim 1$ at AGS energies, 10-15 GeV/nucleon) and increases with A_T
- nuclear transparency is not there!

BARYONS AND STOPPING





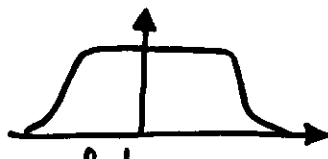
- DEFINING TRANSPARENCY AS:

$$T = \frac{\langle M_p \rangle + \langle M_n \rangle}{A_p}$$

E814 GETS $T = 1/350$ FOR Pb TARGET, WHICH CORRESPONDS TO A MEAN FREE PATH OF $\lambda = 2.4 \text{ fm}$ IN THE LABORATORY.

- AT CERN (SPS ENERGIES, NA35 AND WA80 OBTAIN (FROM BARYON DISTRIBUTIONS) INDICATIONS FOR LESS STOPPING THAN AT 14.6 GeV/N.

- evaluation of energy density ϵ is again "model" dependent:

MODEL	dN/dy	ENERGY DENSITY
ISOTROPIC FIREBALL	 $\sigma_y = 0.88$	$\epsilon_{FB} = \frac{\gamma_{cm} E_T}{V}$
LANDAU MODEL (LONGIT. EXPANSION)	 $\sigma_y \propto \ln \sqrt{s}$	
BJORKEN MODEL (ULTRARELATIVISTIC)	 plateau	$\epsilon_{BJ} = \frac{(dE_T/d\eta)_{max}}{\underbrace{\pi r_0^2 A_p^{2/3}}_{\perp \text{ area}} \tau}$ $\tau \sim 1 \text{ fm}/c$

- **HELIOS** data, taking (arbitrarily) E_T at $\frac{d\sigma}{dE_T} = 10^{-2} \text{ mb}/\text{GeV}$:

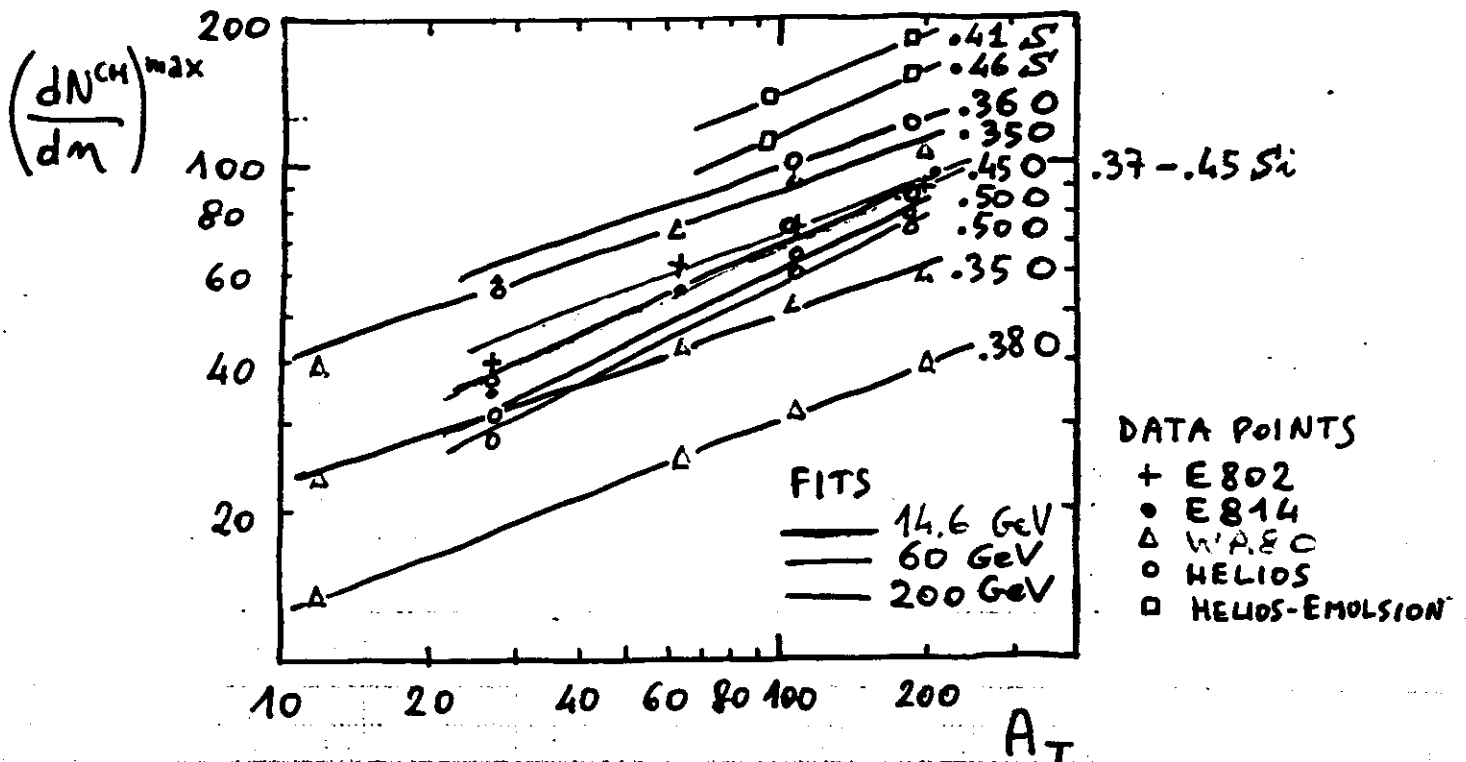
BEAM ENERGY ↓	TARGET →	Al	Ag	W
160-60		2.8	1.8	1.6
		1.2	2.0	2.6
160-200		7.6	5.1	4.6
		1.6	2.6	3.3
325-200		8.1	6.3	5.6
		1.3	2.6	3.3

ϵ_{FB}
 ϵ_{BJ} GeV/f

- large uncertainties, true $\epsilon \approx$ Landau?
- significant increase with E_{BEAM}
- increasing A_p is compensated (in ϵ_{BJ}) by increase of transverse area
- we are reaching (with the most extreme collisions) the hoped for values of ϵ !

PROJECTILE AND TARGET MASS DEPENDENCE

- PARAMETRIZE A_T -DEPENDENCE OF $(dN^{CH}/dm)_{max}$ AS A_T^α :



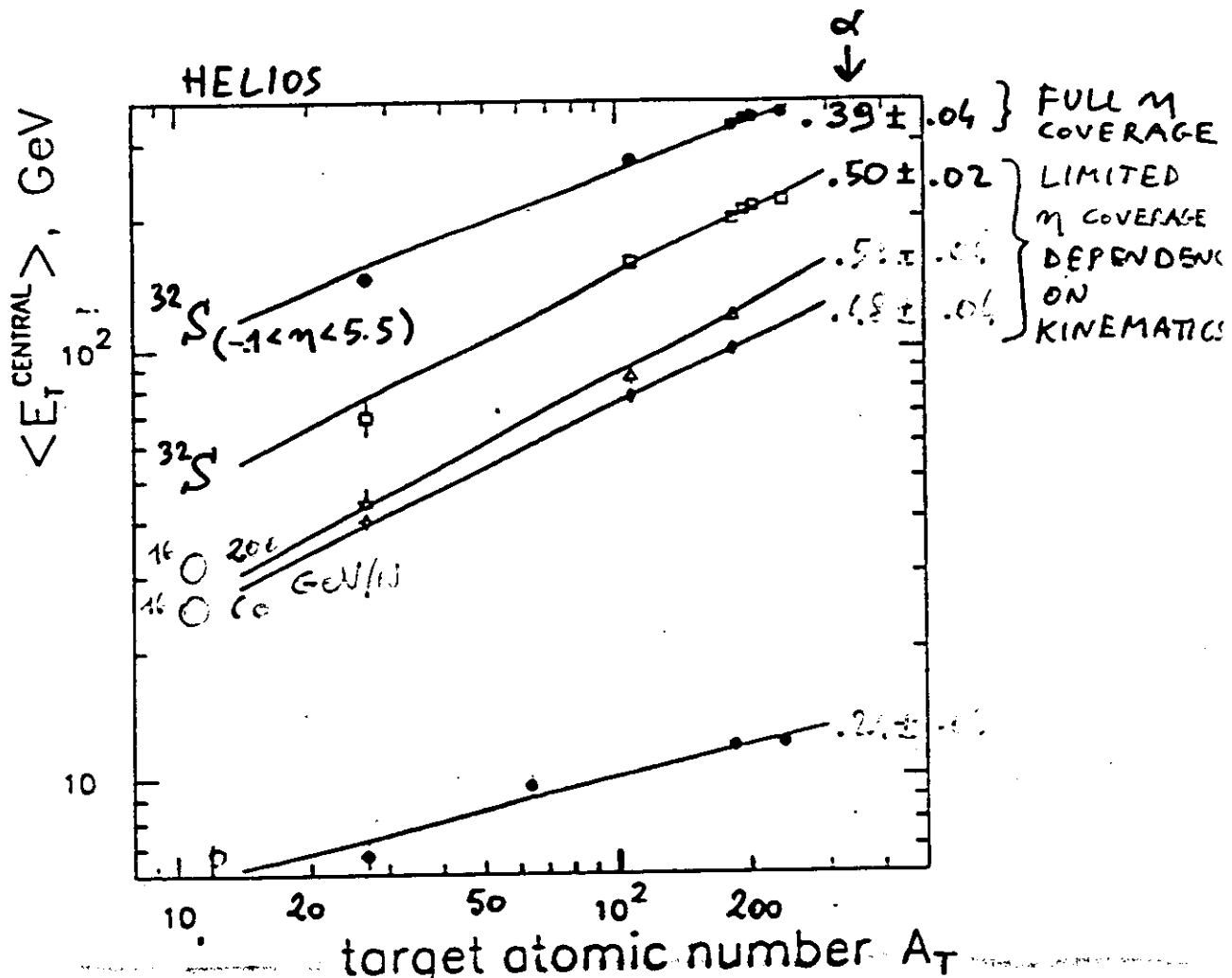
$\alpha \approx 0.35 - 0.50$, WITH NO CLEAR DEPENDENCE ON BEAM ENERGY OR PROJECTILE.

- ▶ MODELS BASED ON NUCLEON-NUCLEON COLLISIONS PREDICT $\alpha = 0.33$, THE LARGER VALUES MIGHT INDICATE RESCATTERING EFFECTS.

- E_T PRODUCTION VS. PROJECTILE MASS A_p : COMPARING ^{16}O AND ^{32}S ON HEAVY TARGETS AN INCREASE OF A FACTOR 1.62 - 1.80 IS OBSERVED.

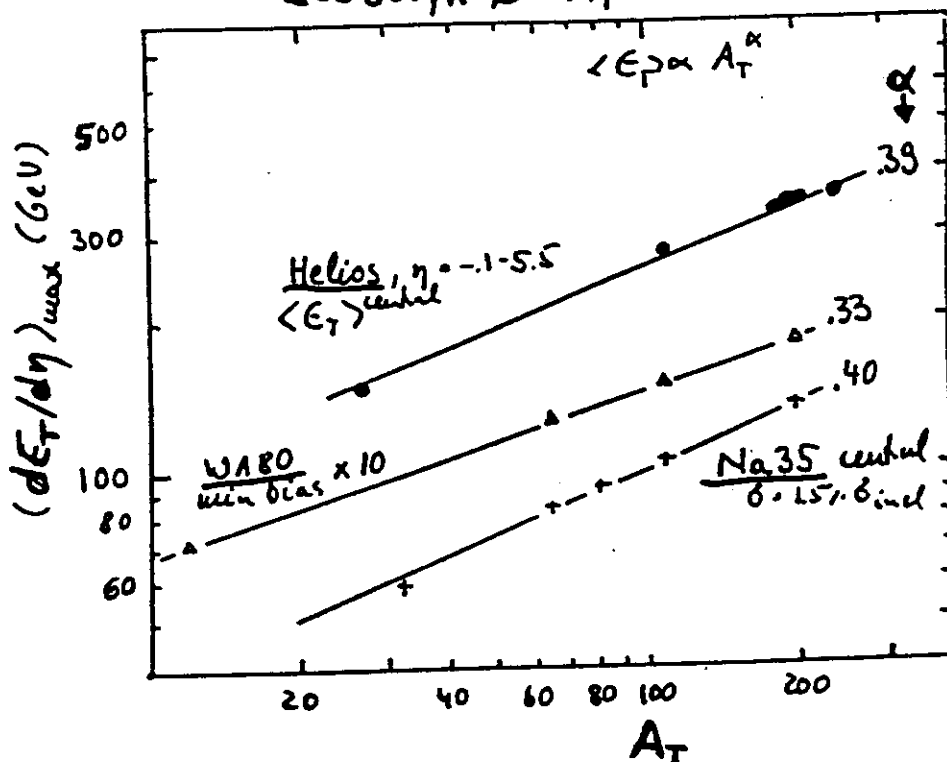
- ▶ SCALING WITH $A_p^{2/3}$ (PROJECTILE TRANSVERSE AREA) WOULD GIVE A FACTOR 1.58, WHILE IF ALL OVERLAPPING NUCLEONS PARTICIPATE ONE GETS $A_p^{5/6}$ SCALING AT HIGH ENERGY, I.E. A FACTOR 1.78.

• E_T PRODUCTION VS. TARGET MASS A_T :



- INCOMPLETE STOPPING! FULL STOPPING WOULD GIVE E_T INDEPENDENT OF A_T FOR LARGE ENOUGH A_T . FULL STOPPING PLUS HYDRODYN. EXPANSION PREDICTS $\alpha = 1/6$.

200 GeV/c $\text{S} + A_T$



IV. P_T DISTRIBUTIONS & PARTICLE RATIOS

- P_T DISTRIBUTIONS ARE EXPECTED TO PROVIDE INFORMATION ON BOTH COLLECTIVE FLOW OF PARTICLES (FOLLOWING THERMALIZATION) AND THE EQUATION OF STATE.
- THE INVARIANT CROSS-SECTION $E d^3\sigma/dp^3$ MAY BE WRITTEN (IGNORING THE y -DEPENDENCE):

$$\frac{1}{P_T} \frac{dN}{dp_T} \quad \text{OR} \quad \frac{1}{m_T} \frac{dN}{dm_T} \quad (m_T^2 = p_T^2 + m^2)$$

FOR A THERMALIZED SYSTEM AT TEMPERATURE T :

$$\frac{1}{P_T} \frac{dN}{dp_T} \sim C m_T^{1/2} e^{-m_T/T}$$

$$\Rightarrow \frac{1}{m_T^{3/2}} \frac{dN}{dm_T} \sim C e^{-m_T/T}$$

IMPLYING THE SAME EXPONENTIAL DISTRIBUTION FOR ALL PARTICLES: m_T SCALING (CONCEPT FROM PP COLLISIONS).

- A COLLECTIVE FLOW (E.G. TRANSVERSE EXPANSION FOLLOWING THE INITIAL LONGITUDINAL EXPANSION IN HYDRODYNAMICAL MODELS) WOULD BREAK THE EXPONENTIAL FORM, AND WOULD AFFECT MORE THE HEAVIER PARTICLES (THEY WOULD GET MORE MOMENTUM $p = mv$ FROM THE SAME COLLECTIVE VELOCITY v).
- IT IS NOT CLEAR THAT m_T SCALING \Rightarrow THERMALIZATION, HOWEVER, SINCE IT APPLIES ALSO TO PP COLLISIONS WHERE THERMALIZATION IS DOUBTFUL.

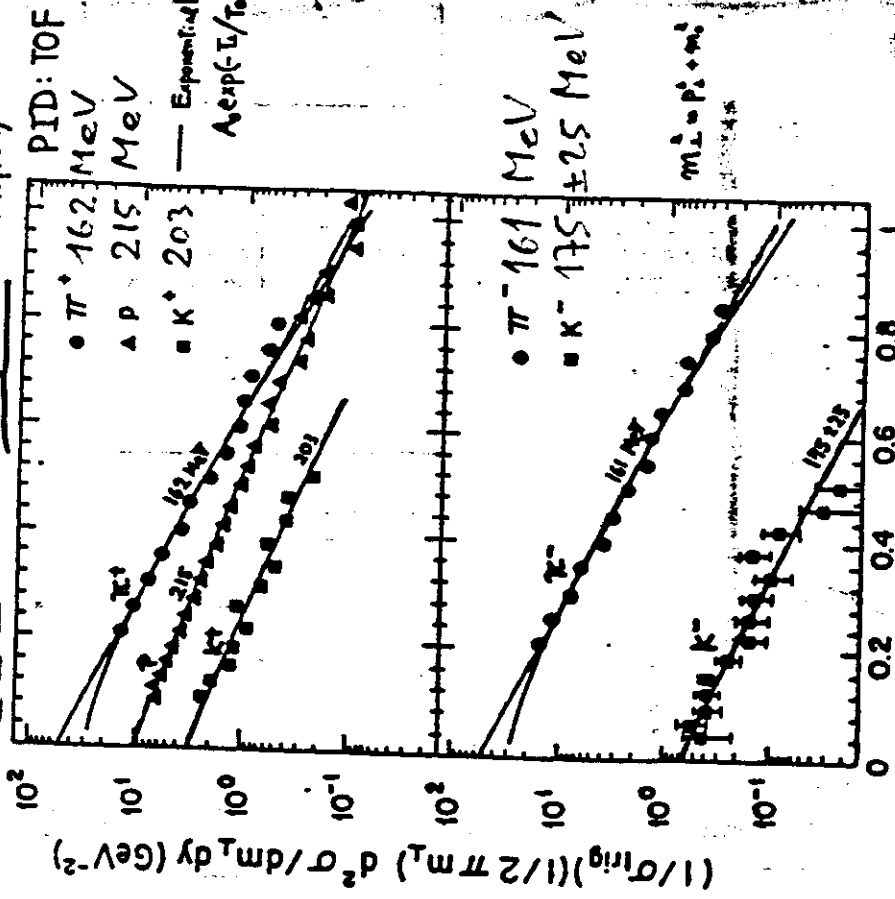
PRL 64(10)249

CENTRAL Si + Au

E802

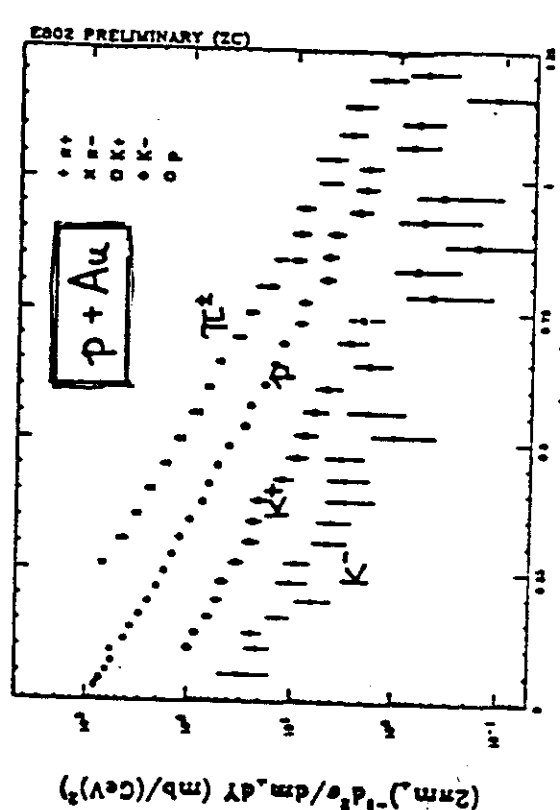
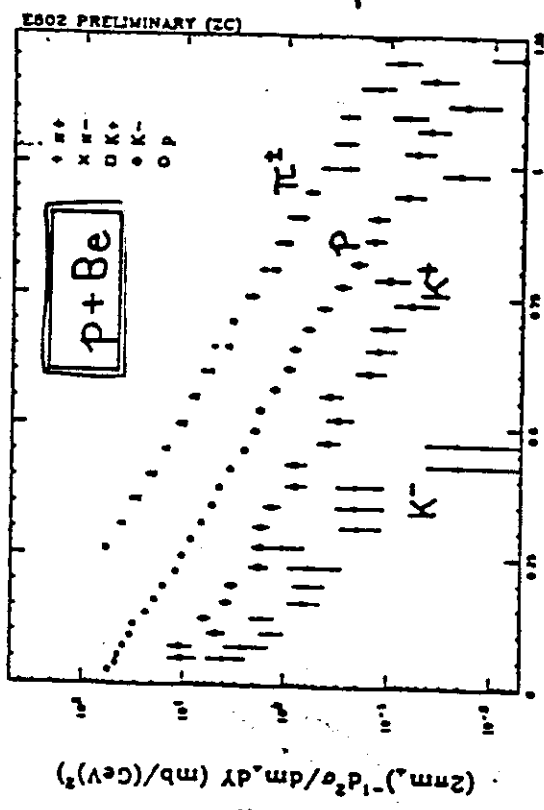
14.6 A-GeV/c ²⁸Si + ¹⁹⁷Au

Central Trigger 1.2 <math>sy < 1.4</math> : Mid rapidity



Particle spectra from 14.6 GeV/c p+Be, p+Au (min. bias)

Extended PID: TOF + GASC
(rekeep up to 50GeV)



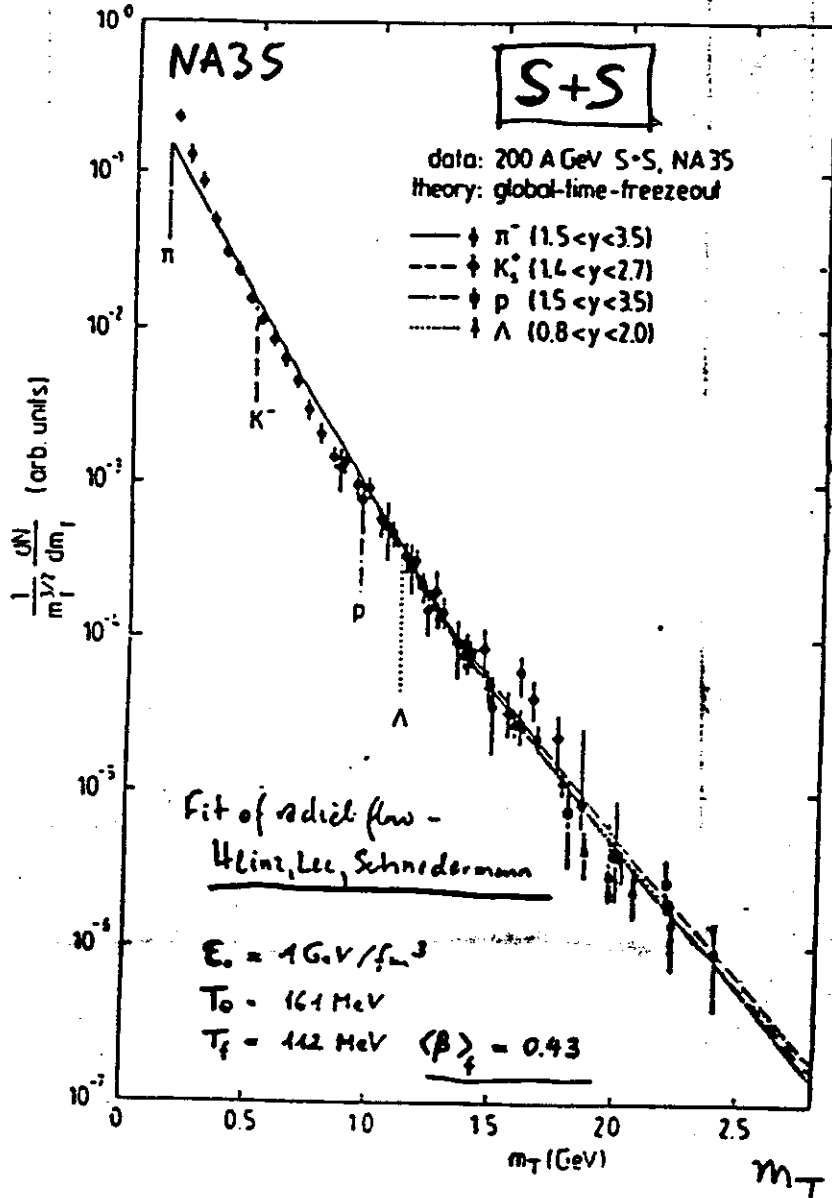
m_T slopes
 are all
 ~ same
 like in p-p
 $T \sim 150 \text{ MeV}$

protons maybe
 flatter?

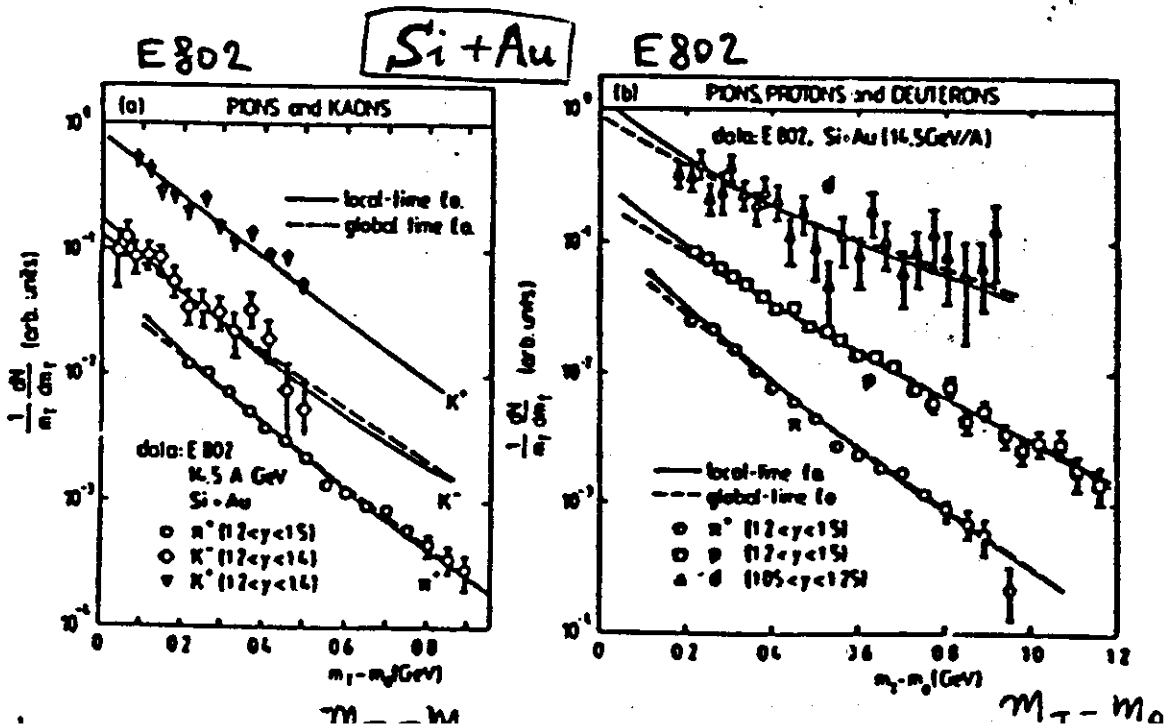
$m_T = m_0$
 m_T slopes are not the same!

● MODELS INCLUDING RADIAL COLLECTIVE FLOW AFTER FREEZE OUT ARE COMPATIBLE WITH DATA

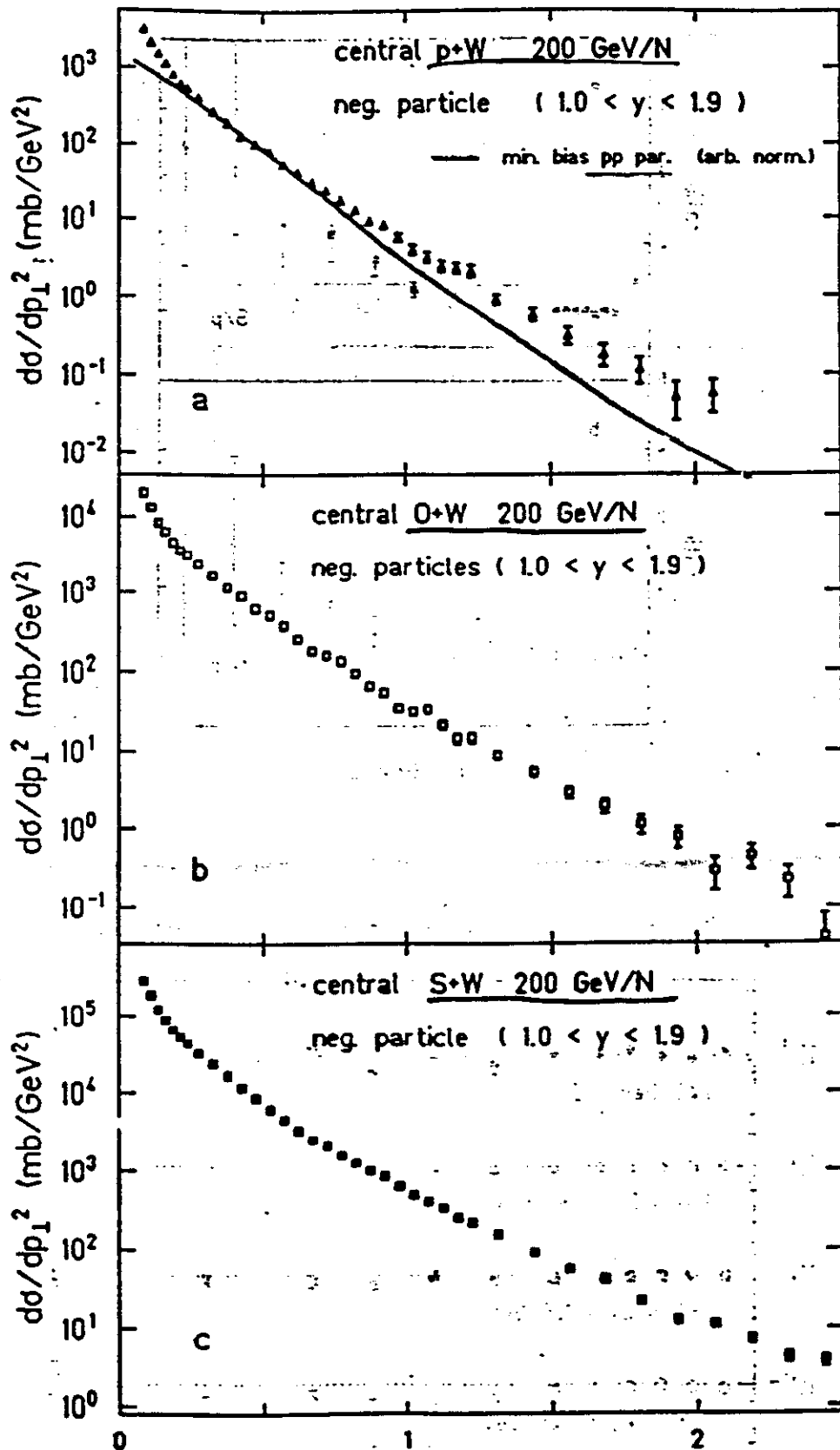
$$\frac{1}{m_T^{3/2}} \frac{dN}{dm_T}$$



pions have curvature at low m_T ;
other particles follow an exponential.



HELIOS NEGATIVE PARTICLES



low p_{\perp} excess
mysterious

high p_{\perp} (> 1.6)
excess which
is well-known
Cronin effect
 $\frac{dN}{d^3p} \propto A^{n(p)}$

interpreted as
FACTIVE PARTICLES
& CATTERING
OR
RESCATTERING
WITH SPECTATOR

soft $\pi^- p_{\perp}$ (GeV/c)
target: rescatt., Δ, N^* decays
central: collective exp.
coll QGP

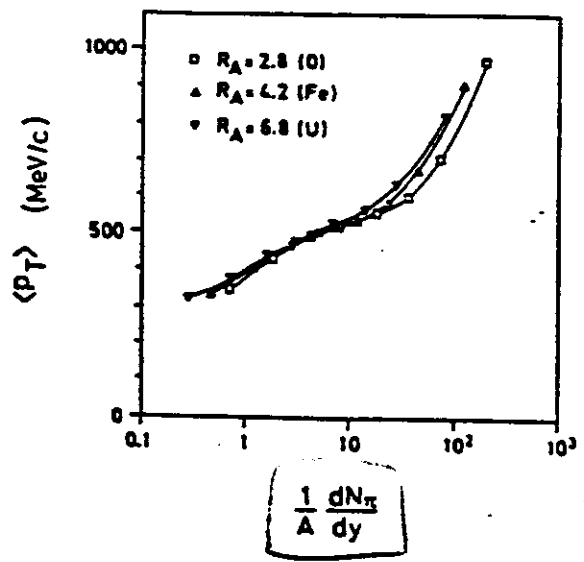
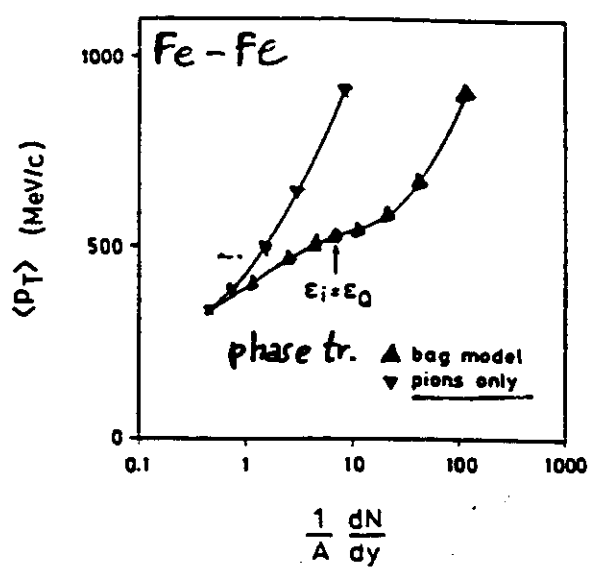
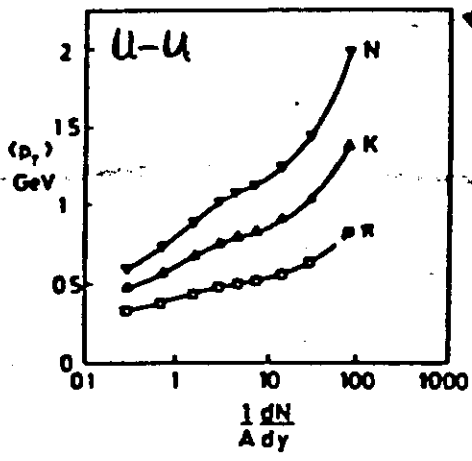


FIG. 6. Average p_T with and without phase transition. In the latter case the matter is assumed to be produced as hot pion gas. At the point indicated by $\epsilon_i = \epsilon_0$, pure plasma state at T_c is reached at τ_c .

FIG. 7. Average p_T as a function of normalized multiplicity ($1/A dN_T/dy$) for U-U ($R_A = 6.8$), Fe-Fe ($R_A = 4.2$), and O-O ($R_A = 2.8$ fm) collisions.

APPROXIMATE SCALING VS. A
 IF dN/dy IS DIVIDED BY A.



STRONGER $\langle p_T \rangle$
 GROWTH FOR
 HEAVIER PARTICLES

► INFORMATION ON THE EQUATION OF STATE IS OBTAINED BY PLOTTING $\langle p_T \rangle$ (RELATED TO TEMPERATURE) VS dN/dy (RELATED TO ENTROPY DENSITY).

► THE QGP (WITH A BAG MODEL EQUATION OF STATE) PRODUCES LOWER $\langle p_T \rangle$ PARTICLES THAN A PION GAS, FOR THE SAME RAPIDITY DENSITY dN/dy .

► THE EXPANSION WILL INCREASE $\langle p_T \rangle$ BEYOND THERMAL VALUES, SOFTENING THE DIFFERENCE BETWEEN QGP AND HADRON GAS.

E-735 (FNAL)

$\bar{p}p$ at $\sqrt{s} = 1.8$ TeV

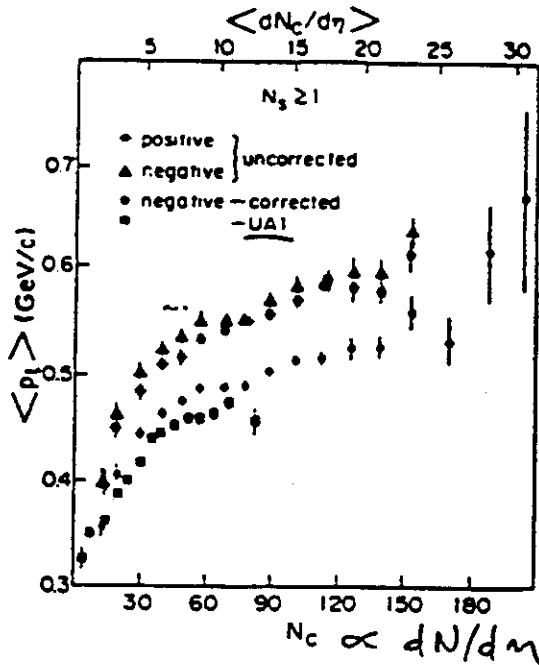


FIG. 4. $\langle p_t \rangle$ as a function of N_c and $\langle dN_c/d\eta \rangle$ for all positive tracks and all negative tracks averaged over the interval $0.15 \text{ GeV}/c < p_t < 3.0 \text{ GeV}/c$. The corrected $\langle p_t \rangle$ of negative particles includes unobserved particles with $p_t < 0.15 \text{ GeV}/c$ (see text). The last few uncorrected data points are omitted for clarity. The UA1 data (Ref. 5) are from $\sqrt{s} = 540 \text{ GeV}/c$.

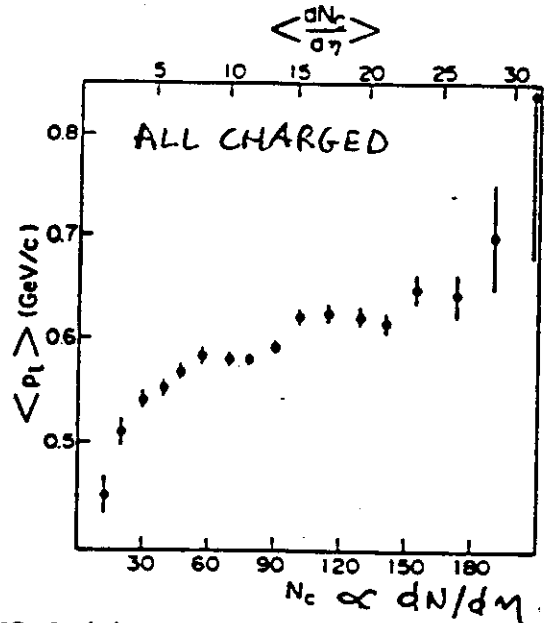


FIG. 5. $\langle p_t \rangle$ as a function of N_c and $\langle dN_c/d\eta \rangle$ for all charged particles with $N_c \geq 2$, averaged over the interval $0.15 \text{ GeV}/c < p_t < 3.0 \text{ GeV}/c$.

plateau = mixed phase?

"plateau" values for $\langle p_t \rangle$

$\pi \sim 375 \text{ MeV}/c$

$K \sim 525$

$\bar{p} \sim 625$
 $\langle dN_c/d\eta \rangle$

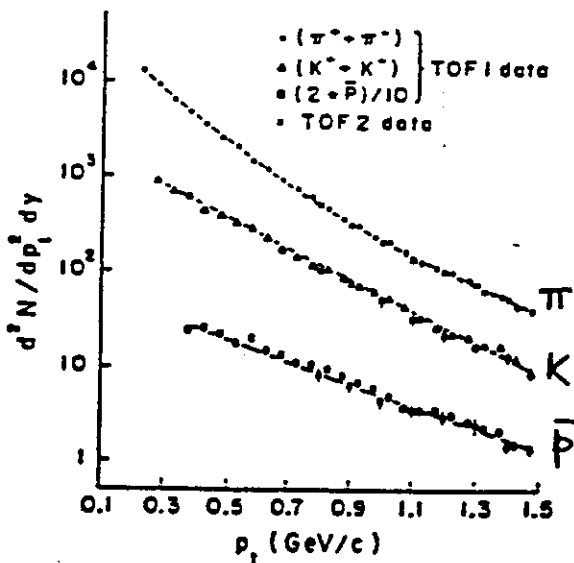


FIG. 1. Plot of inclusive $d^2N/dp_t^2 dy$ as a function of p_t for pions, kaons, and antiprotons. The particles are mass identified using two independent hodoscopes, TOF1 and TOF2 (see text), and the results from both detectors are shown as a consistency check. The curves shown correspond to fits (described in the text) in the regions $0.2 < p_t < 1.5 \text{ GeV}/c$ (pions), $0.25 < p_t < 1.5 \text{ GeV}/c$ (kaons), and $0.35 < p_t < 1.5 \text{ GeV}/c$ (antiprotons).

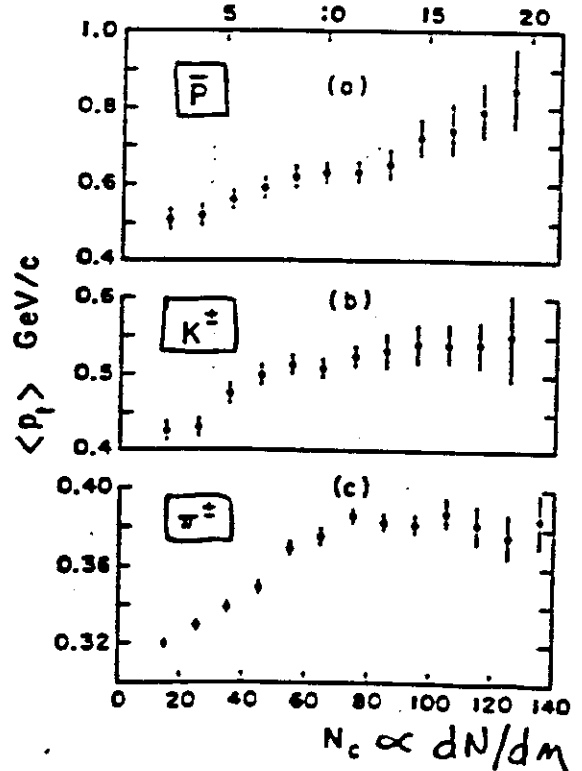
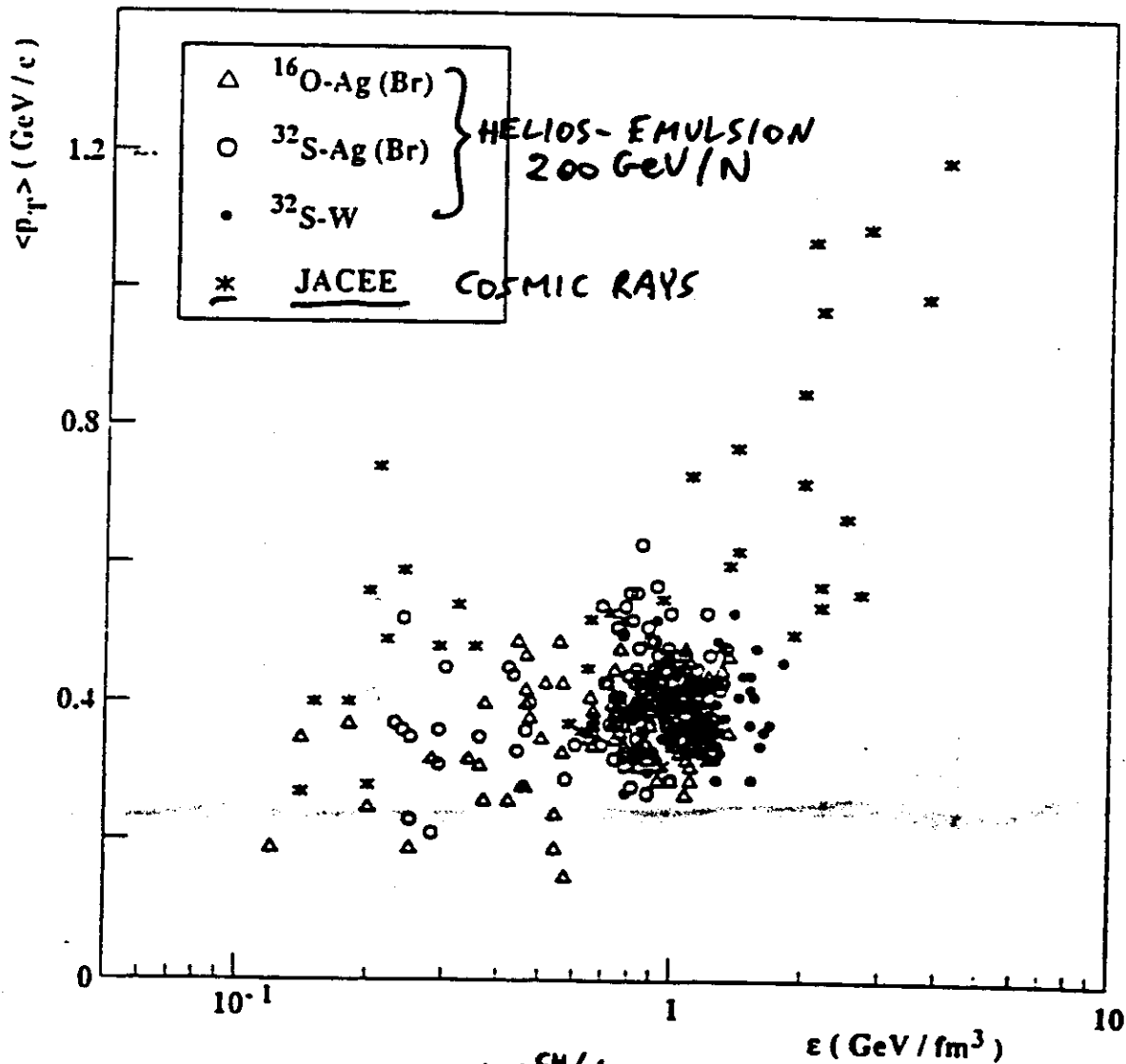


FIG. 2. (a)-(c) Plots of $\langle p_t \rangle$ vs $dN_c/d\eta$ (or N_c) for \bar{p} , kaons, and pions, respectively, for particles with $p_t < 1.5 \text{ GeV}/c$.



$$\epsilon = \frac{3}{2} \frac{\langle m_T \rangle dN^{ch}/dm}{\pi R_0^2 A_P^{2/3} \cdot 2T_0}$$

Rjackson formula

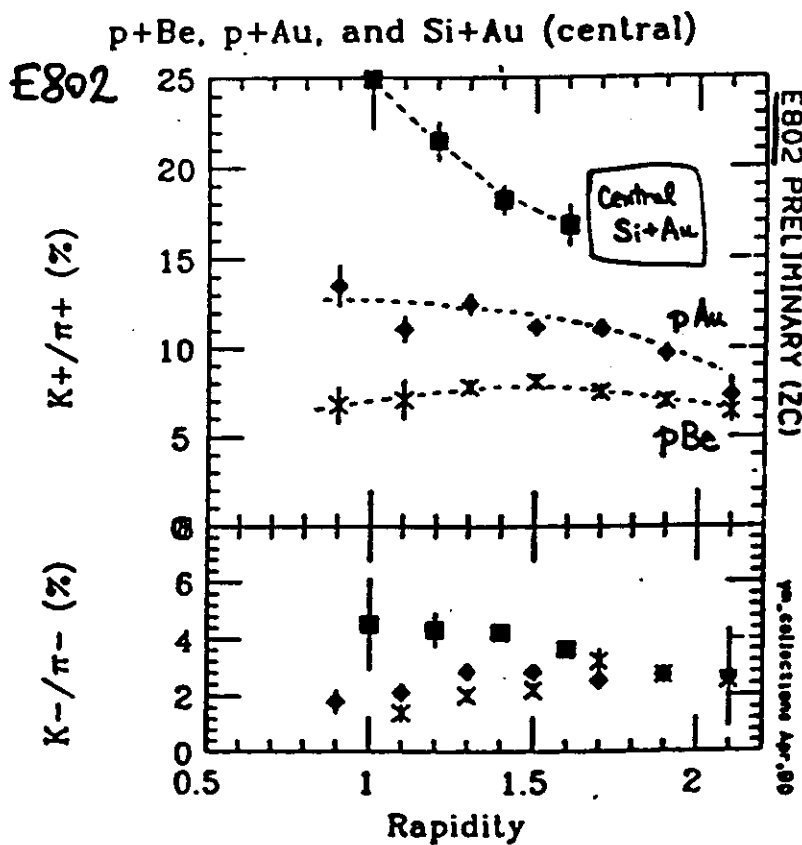
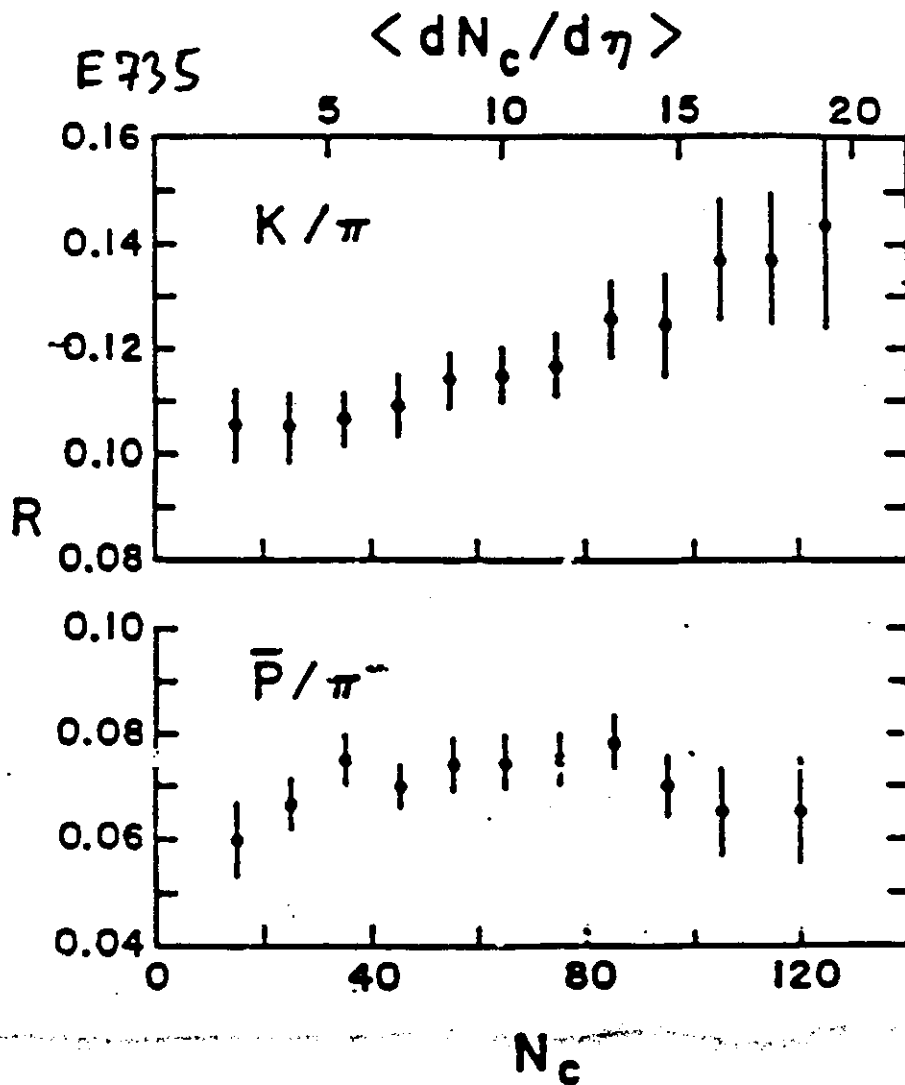
$$\langle m_T \rangle = \sqrt{\langle p_T \rangle^2 + m_\pi^2}$$

$$T_0 = 1 \text{ fm/c}$$

- ▶ HELIOS-EMULSION DATA DO NOT REACH AS HIGH ϵ AS JACEE DATA
- ▶ JACEE DATA SEEM TO RISE TOO RAPIDLY TO FIT QGP; HOWEVER AN IDEAL PION GAS FIT GIVES UNREALISTICALLY HIGH TEMPERATURE.

PARTICLE RATIOS

- STRANGE PARTICLES ARE A VERY INDIRECT PROBE OF QGP SINCE THEY ARE FORMED RATHER LATE; A HADRON GAS HAS STRANGENESS ABUNDANCES VERY SIMILAR TO THE QGP (UNLESS THERE ARE NON-EQUILIBRIUM EFFECTS).
 - IN ANY CASE, K/π RATIOS PROVIDE INFORMATION ABOUT THE CHEMICAL EQUILIBRIUM OF THE HADRON GAS, AND CAN BE USED TO EXTRACT THE TEMPERATURE AND BARYON DENSITY AT DECOUPLING.
 - ▶ K^+/π^+ has been measured to increase gradually from pBe to pAu to central SiAu collisions (E802) while K^-/π^- does not increase much. → FIG.
 - ▶ These data are fitted by a Chemically Equilibrated Hadron gas model with $T \sim 105$ MeV and $n_B \sim 0.05$ baryons/fm³ → FIG.
 - ▶ At CERN energies, NA35 and WA85 have measured Λ , $\bar{\Lambda}$, K_S^0 production; WA85 also measured Ξ^- and Ξ^0 production. Large ratios $\bar{\Lambda}/\Lambda$ and $\bar{\Xi}^-/\Xi^0$ have been reported:
$$0.16 \leq \bar{\Lambda}/\Lambda \leq 0.39, \quad 0.36 \leq \bar{\Xi}^-/\Xi^0 \leq 0.5$$
 - ▶ The CERN data require higher values of parameters:
 $T \sim 180$ MeV, $n_B \sim 0.12$ baryons/fm³
in the CLEGG model.
- So far, a consistent picture is missing.



CENTRAL Si+Au

$$\left\langle \frac{K^+}{\pi^+} \right\rangle = 19\%$$

$$\left\langle \frac{K^-}{\pi^-} \right\rangle = 3.6\%$$

CLEYMANS QM '80 CLEHG Model $\left. \begin{array}{l} \text{resonance prod.} \\ \text{baryon repulsion} \end{array} \right\}$

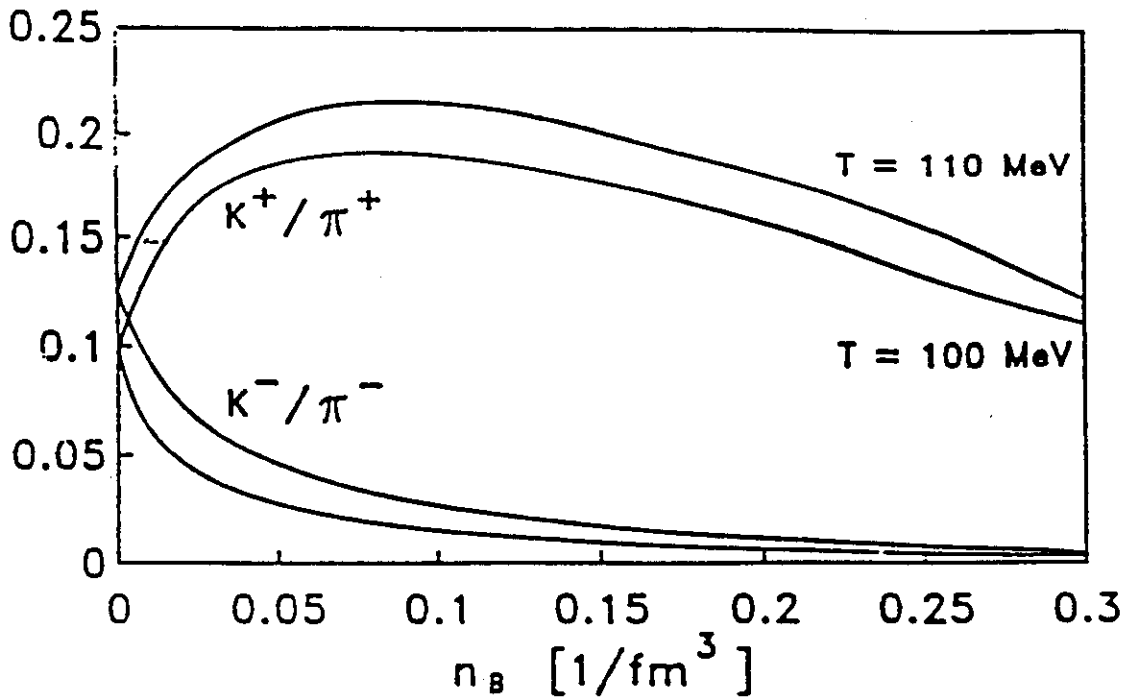


Figure 4: Dependence of the K/π ratios on the baryon density for different values of the temperature T .

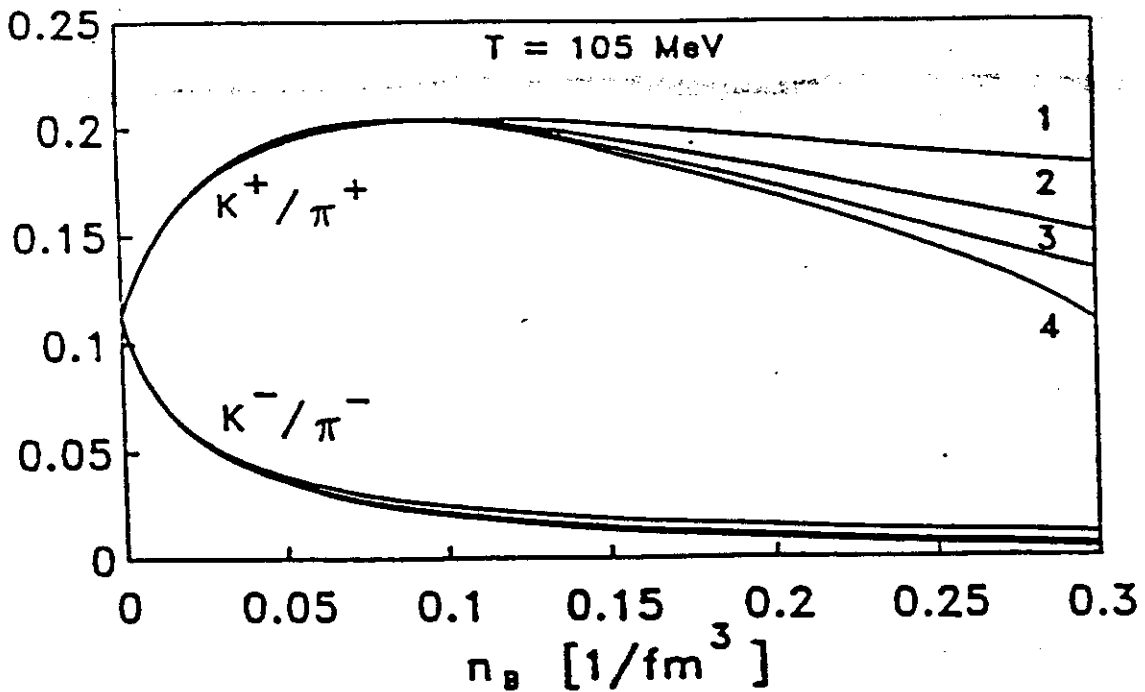


Figure 5: Dependence of the K/π ratios on different choices for the volume corrections: no corrections (1), purely geometric (2), depending on the energy density (3) and on the baryon density (4).

basic idea: $K^+/\pi^+ \sim \frac{\bar{s}u}{\bar{d}u} \sim \frac{\bar{s}}{\bar{d}} \sim \frac{e^{-m_s/T}}{e^{-\mu/T}}$ $\mu = \text{chemical potential}$

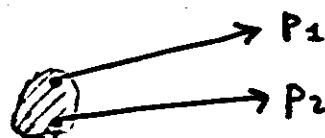
$K^-/\pi^- \sim \frac{e^{-m_s/T}}{e^{\mu/T}}$

$\therefore \dots$ (by increasing n_B)

V. PION INTERFEROMETRY

- PRINCIPLE: WHEN 2 IDENTICAL BOSONS: (E.G., 2 PIONS) ARE DETECTED, THE BOSE-EINSTEIN CORRELATION IN 4-MOMENTUM SPACE HAS A MAGNITUDE INVERSELY PROPORTIONAL TO THE SIZE OF THE SOURCE IN COORDINATE SPACE. ONE HAS TO MEASURE:

$$C_2(p_1, p_2) = \frac{N_2(p_1, p_2)}{N(p_1)N(p_2)}$$



- PRACTICAL DIFFICULTIES:
 - i) RESONANCES
 - ii) FINAL STATE INTERACTIONS (NEUTRAL BOSONS ARE BETTER!)
→ GAMOW CORRECTION
 - iii) BACKGROUND → USE EVENT MIXING TO ESTIMATE IT
 - iv) SPACE-TIME GEOMETRY OF COLLISION → USE MODELS

- THE SIMPLEST MODEL IS A SOURCE DESCRIBED BY GAUSSIANS SEPARABLE IN SPACE AND TIME:

$$C_2(Q_T, Q_L) = 1 + \lambda \exp(-Q_T^2 R_T^2 / 2) \exp(-Q_L^2 R_L^2 / 2)$$

WITH Q_L (Q_T) = LONGITUDINAL (TRANSVERSE) MOMENTUM DIFFERENCE, λ = CHAOTICITY PARAMETER,

R_L (R_T) = LONGITUDINAL (TRANSVERSE) SOURCE SIZE.

- ▶ NA35 RESULTS INDICATE AN INCREASE OF R_T AND R_L FOR π^- COMING FROM THE CENTER-OF-MASS REGION;
 R_T HAS VALUES OF MORE THAN TWICE THE TRANSVERSE PROJECTILE SIZE.
THIS WOULD INDICATE A LARGE-RADIUS, NEARLY SPHERICAL THERMALIZED SOURCE IN THE CENTRAL REGION.

31 March 1988

$^{16}\text{O} + \text{Au}$
200 GeV/N

105 central
events

($E_{\text{ZDC}} < 300 \text{ GeV}$)

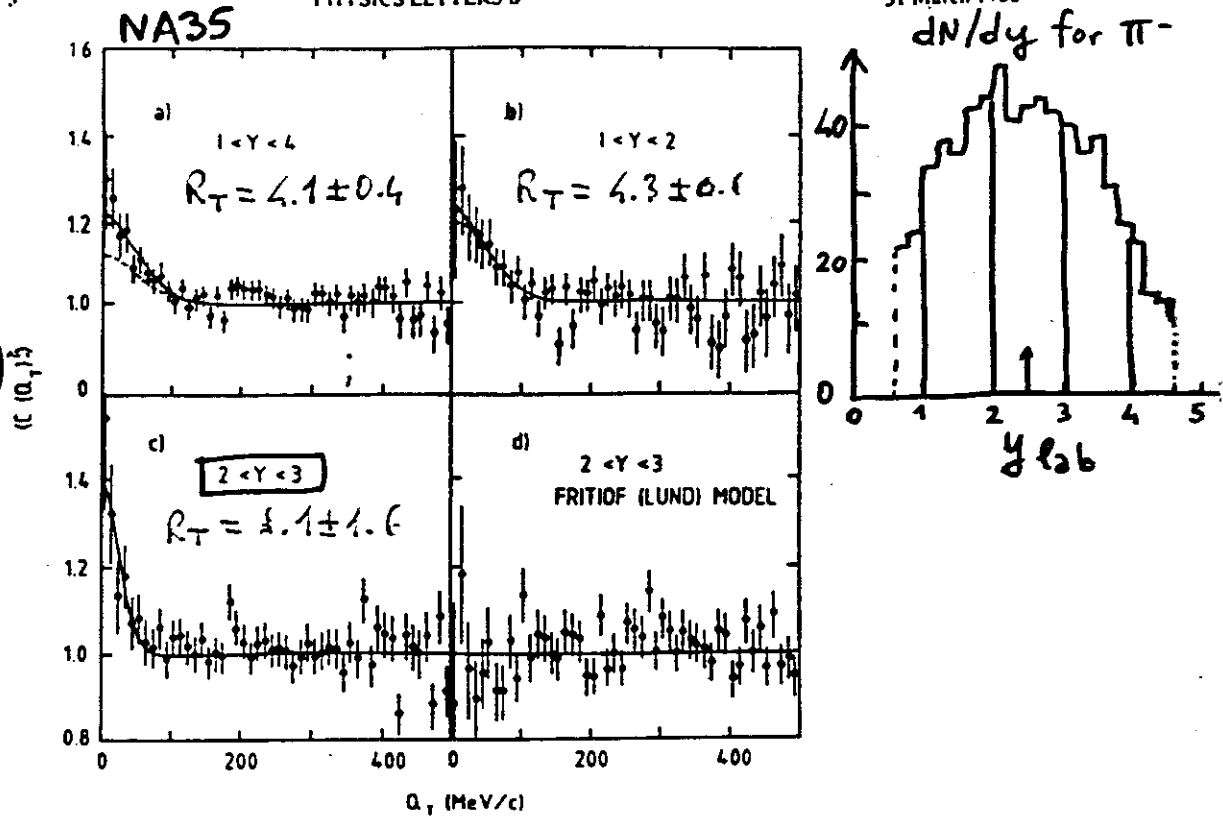
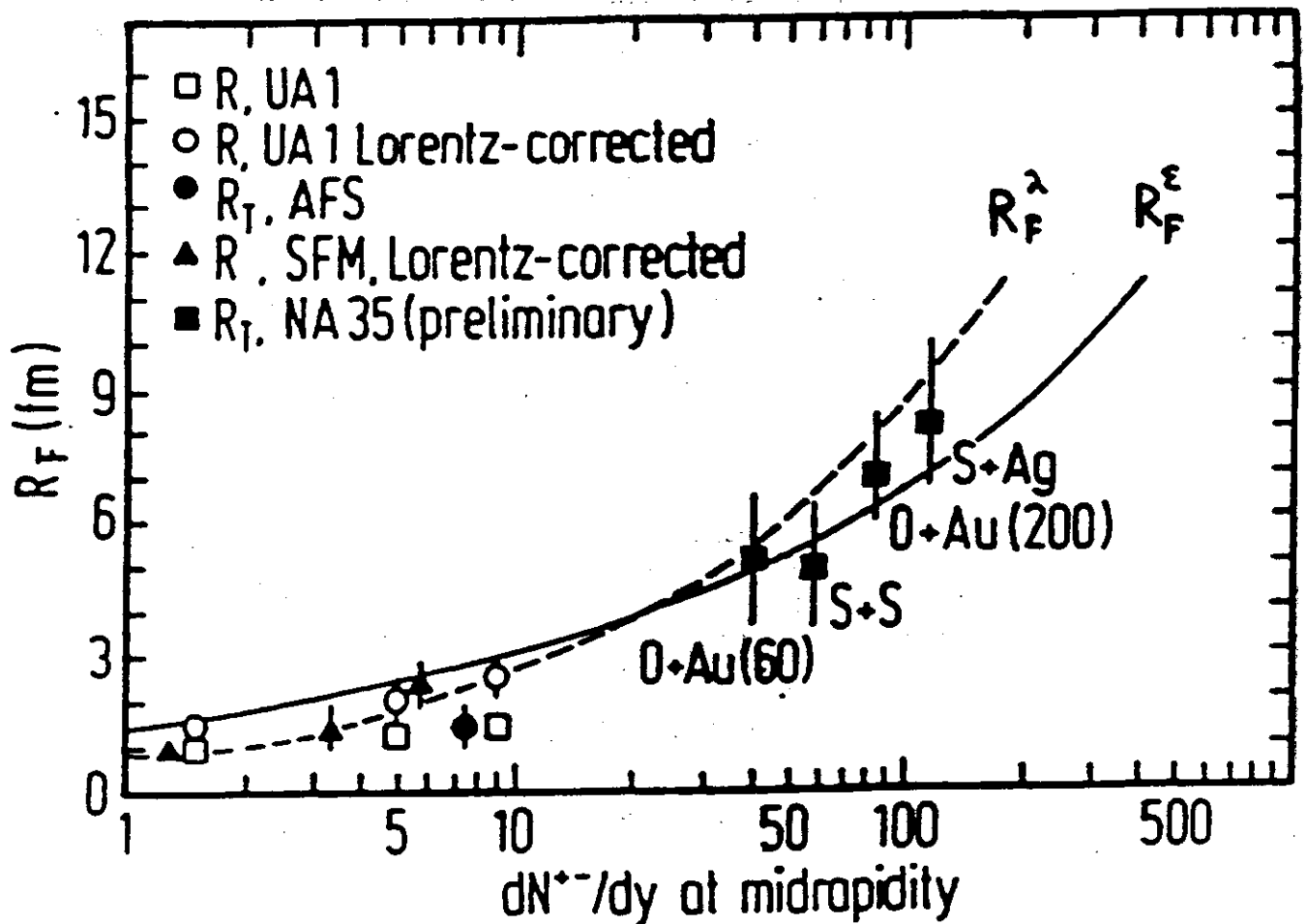
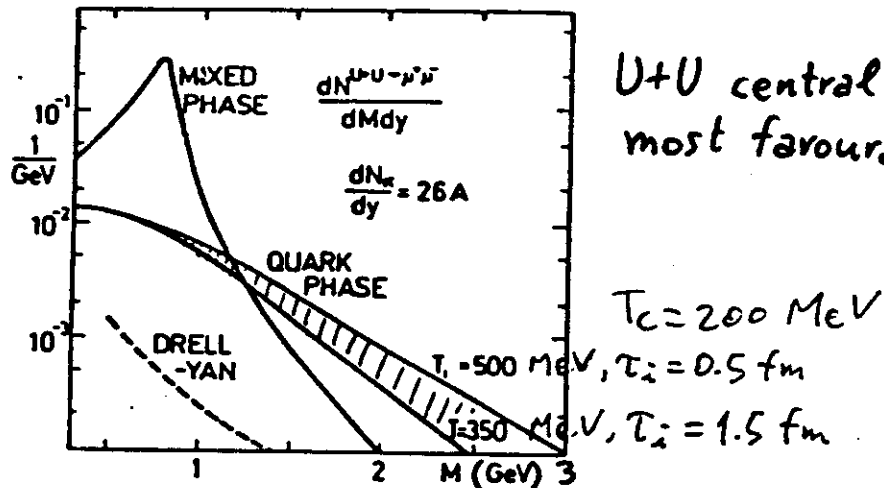


Fig. 2. Correlation function projected on to the Q_T -axis (for pairs with $Q_L < 100 \text{ MeV}/c$) for different rapidity intervals: (a) $1 < \eta < 4$, (b) $1 < \eta < 2$, and (c) $2 < \eta < 3$, data; (d) $2 < \eta < 3$, Fritiof calculation. The projected gaussian fit is shown (solid curve) for each case, and in (a) the dashed curve shows the fit to the non-Gamow-corrected correlation function.



VI. DILEPTONS

KAJANTIE et al.



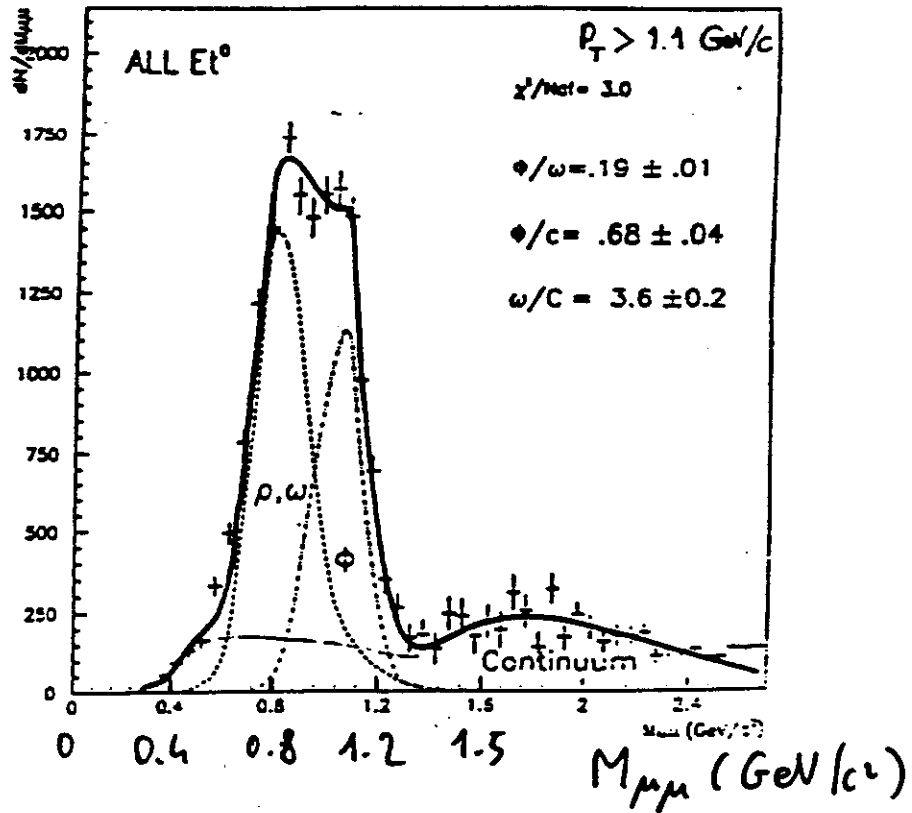
U+U central collisions most favourable case!

Figure 11 Mass distribution of dileptons at $y \approx 0$ from two flows with the same dN/dy but different T_c .

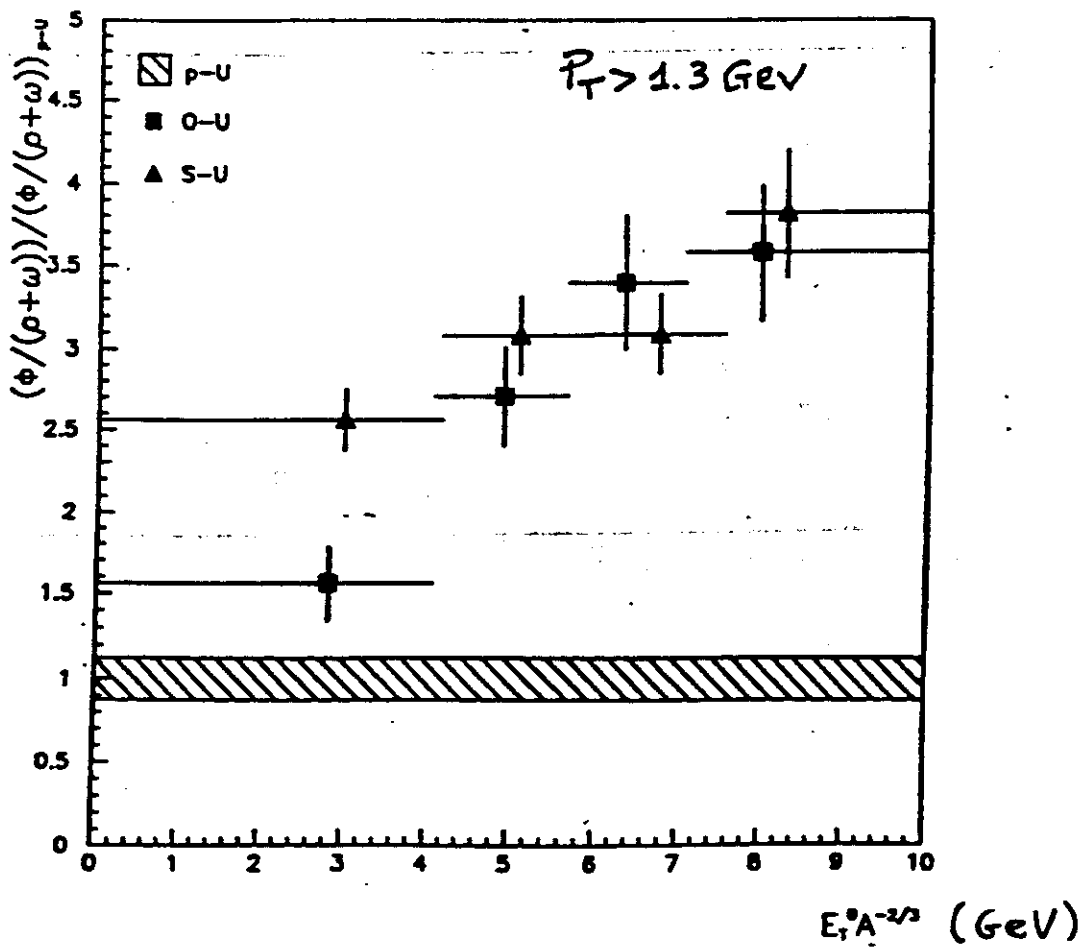
- ▶ DILEPTONS ARE EXPECTED FROM THE QGF PHASE WITH $1 \lesssim M \lesssim 3 \text{ GeV}$ (RATE $\propto (dN^\pi/dy)^2$), AND FROM THE MIXED PHASE WITH $M \approx 1 \text{ GeV}$ AFTER THE MATTER HAS COOLED DOWN TO T_c .
- ▶ NO EVIDENCE HAS BEEN REPORTED SO FAR WITH ^{16}O AND ^{32}S PROJECTILES, BUT DATA ARE STILL TOO PRELIMINARY
- NA38 FINDS AN ENHANCEMENT OF ϕ PRODUCTION W.R.T. ρ, ω IN O-U, S-U COLLISIONS (COMPARED TO P-U COLLISIONS). → FIG.
- ▶ THE ENHANCEMENT HAS BEEN INTERPRETED QUANTITATIVELY BY POSTULATING THAT THE ϕ ONLY REACHES CHEMICAL EQUILIBRIUM IN DENSE NUCLEAR MATTER (MORE RESCATTERING), WHILE THE ρ AND ω MESONS REACH ALWAYS CHEMICAL EQUILIBRIUM, BEING MADE OF LIGHT u, d QUARKS (Koch, Heinz and Pišút).

NA38

S-U 200 GeV/A



$\phi/(\rho+\omega)$ RATIO



J/ψ SUPPRESSION IN QGP (Matsui & Satz, 1986)

- DECONFINEMENT IS A CONSEQUENCE OF COLOR CHARGE SCREENING, CHANGING THE VACUUM POTENTIAL $V_0(r)$ OF A $q\bar{q}$ PAIR INTO:

$$V(r) = V_0(r) e^{-r/r_D} \quad (r_D = \text{Debye radius})$$

- BOUND STATES OF HEAVY QUARKS ($c\bar{c}$, $b\bar{b}$), HAVING A SMALL BOHR RADIUS, SURVIVE INSIDE QGP UNLESS T IS SUCH THAT $r_D < r_{\text{Bohr}}$
- IF QGP IS FORMED, $c\bar{c}$ ($b\bar{b}$) PAIRS "FLY APART" AND CANNOT COMBINE INTO J/ψ (Υ) UNTIL HADRONIZATION, WHEN THE CHANCE OF FINDING A c (b) PARTNER IS LOWER.

⇒ J/ψ PRODUCTION SHOULD BE SUPPRESSED IN CENTRAL COLLISIONS COMPARED TO PERIPHERAL COLLISIONS, AND MORE SUPPRESSED AT LOW $P_T(\text{J}/\psi)$ SINCE AT HIGH P_T THE $c\bar{c}$ PAIR CAN EASILY ESCAPE THE PLASMA.

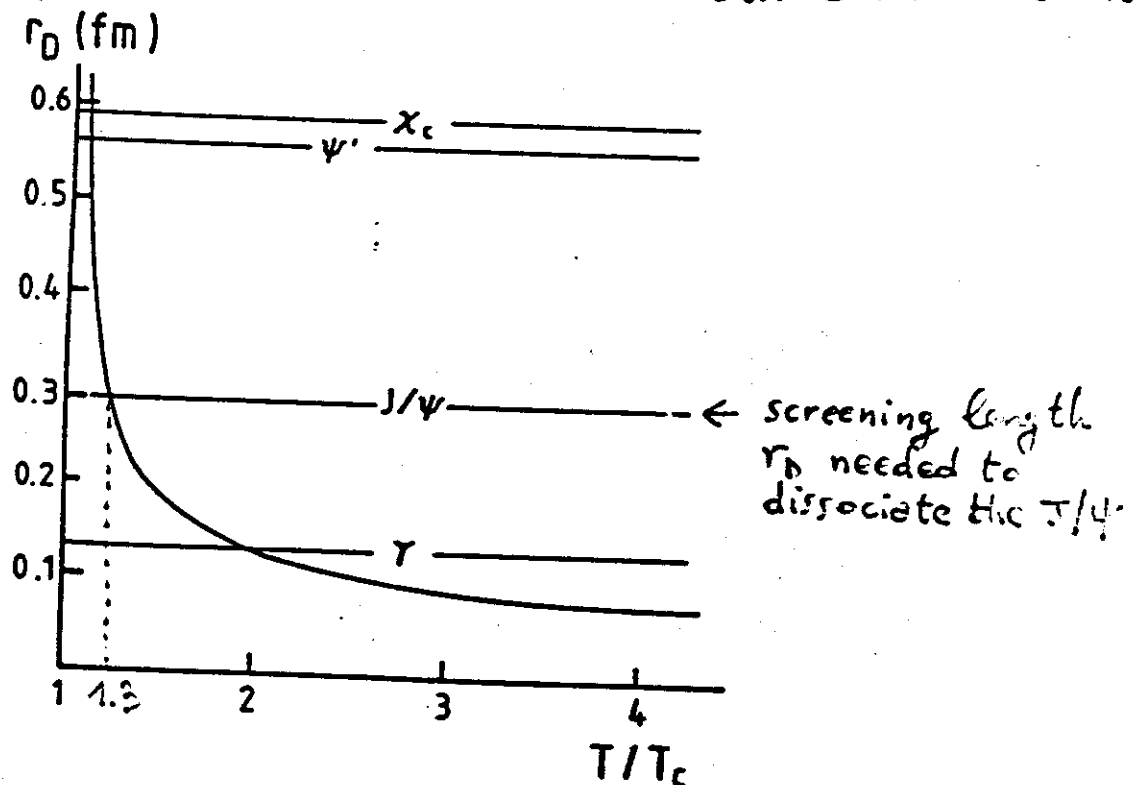
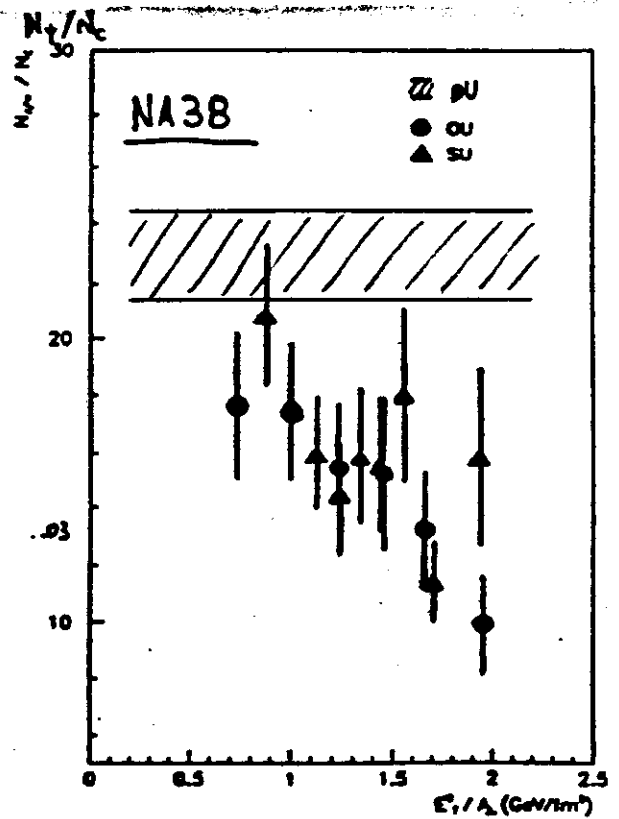
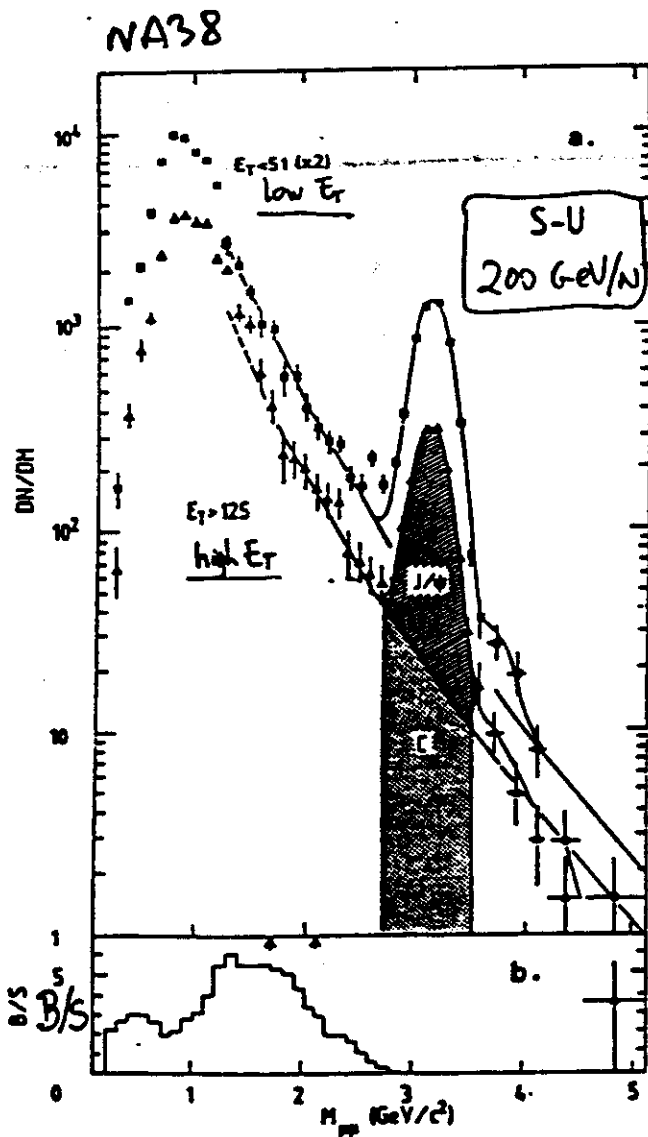


Fig. 5: Screening lengths r_D as function of the temperature, together with the dissociation values of some heavy quark bound states. From Ref. 11, Ref. 13 and Ref. 16.

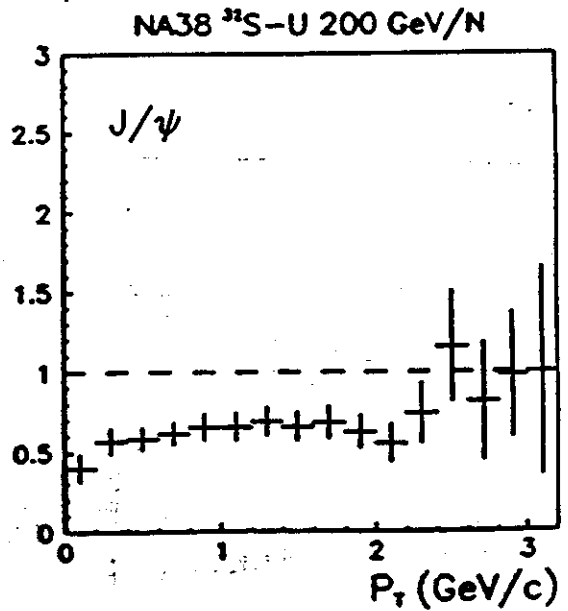
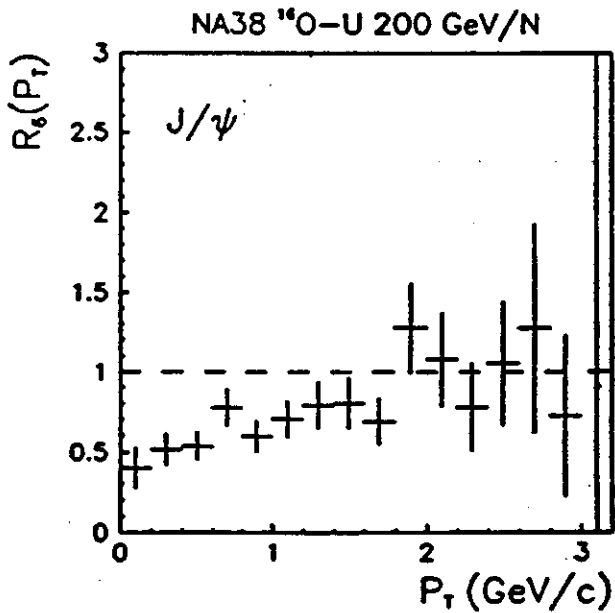
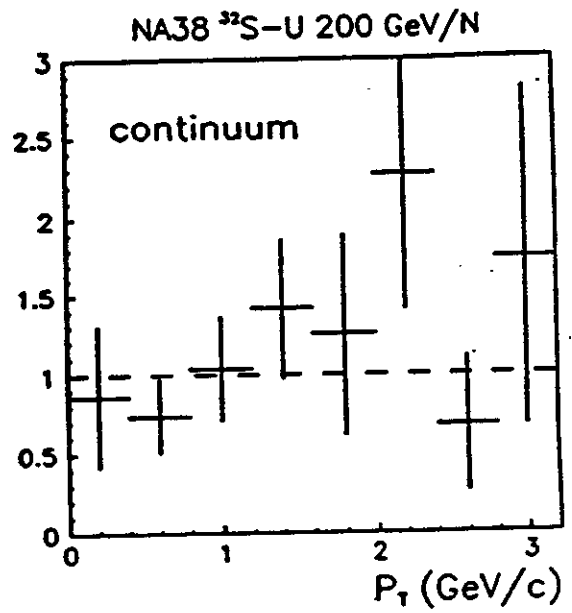
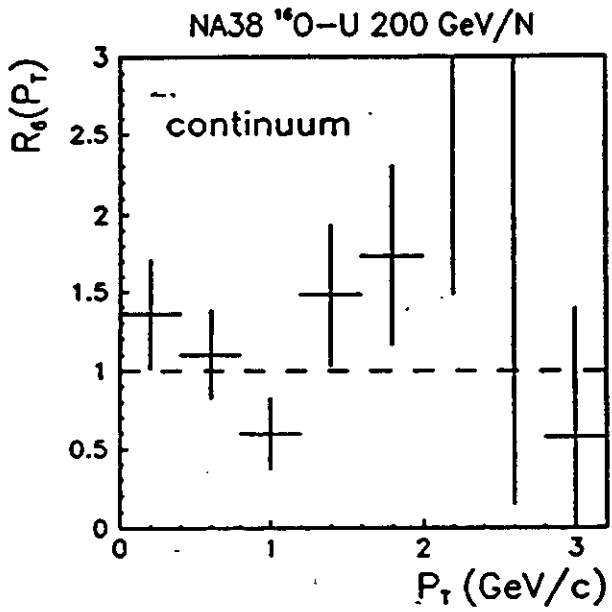
▶ NA38 OBSERVES J/ψ (AND ψ') SUPPRESSION IN HIGH E_T D-U AND S-U COLLISIONS, WHILE NO EFFECT IS SEEN IN P-U.

▶ THE PREDICTED P_T -DEPENDENCE OF THE SUPPRESSION IS OBSERVED AND AGREES QUANTITATIVELY WITH THE MODEL.

▶ ALTERNATIVE EXPLANATIONS, ESSENTIALLY BASED ON J/ψ ABSORPTION IN DENSE HADRONIC MATTER, PREDICT A DIFFERENT P_T -DEPENDENCE AND REQUIRE VERY HIGH HADRON DENSITIES.



NA38



CONCLUSIONS

1. The energy density ϵ has the right order of magnitude to form QGP in "extreme" collisions
2. The stopping power is still high at 200 GeV/N
3. Global features of collisions are essentially understood with simple geometrical considerations
4. THERE IS A POSSIBLE INDICATION OF A MIXED PHASE FROM $\langle p_T \rangle$ vs. dN/dy
5. THERE IS EVIDENCE FOR A LARGE, THERMALIZED SYSTEM FROM 2π INTERFEROMETRY
6. J/ψ SUPPRESSION HAS BEEN ESTABLISHED IN O-U, S-U COLLISIONS, ALTERNATIVE MECHANISMS DON'T REPRODUCE QUANTITATIVELY THE EFFECT

MORE WORK MUST BE DONE ON:

- LOW MASS DILEPTONS NA34, NA45
 - K/π , $\bar{\Lambda}/\Lambda$, \bar{E}/E RATIOS WA85
 - INTERFEROMETRY NA44
- ⇒ LARGER VOLUMES Pb (CERN), Au (BNL) beam.
- ⇒ LARGER ENERGY DENSITY RHIC, LHC

